PRELIMINARY MODELS FOR SCALING POWER SPECTRAL DENSITY FUNCTION OF EARTHQUAKE GROUND MOTIONS

By

BIDISHA DE

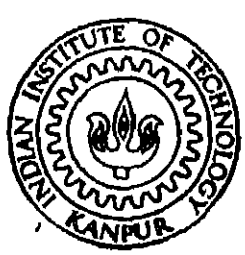

DEPARTMENT OF CIVIL ENGINEERING

INDIAN INSTITUTE OF TECHNOLOGY KANPUR

JUNE, 1997

PRELIMINARY MODELS FOR SCALING POWER SPECTRAL DENSITY FUNCTION OF EARTHQUAKE GROUND MOTIONS

A Thesis Submitted

in Partial Fulfilment of the Requirements

for the Degree of

MASTER OF TECHNOLOGY

by

Bidisha De

to the

DEPARTMENT OF CIVIL ENGINEERING

INDIAN INSTITUTE OF TECHNOLOGY KANPUR

June 1997

CE-1997-M-DE-PRE

CERTIFICATE

It is certified that the work contained in the thesis entitled "**Preliminary Models for Scaling Power Spectral Density Function of Earthquake Ground Motions**" by "**Bidisha De**" has been carried out under my supervision and that this work has not been submitted elsewhere for a degree.

Vinay 24.6.97

(VINAY KUMAR GUPTA)
Associate Professor
Department of Civil Engineering
Indian Institute of Technology
Kanpur

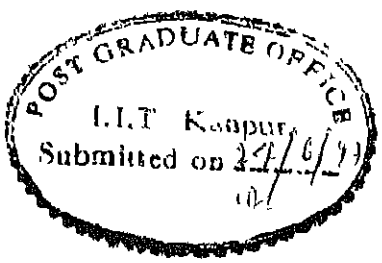

ACKNOWLEDGEMENTS

I am thankful to my advisor, Dr V K. Gupta, for his able guidance and constant support throughout my tenure of about two years in IIT(K). I am also grateful to Dr. Debashish Kundu for the selfless help he has always rendered during the course of my thesis work

I also consider myself fortunate to have had the company of the '95 Structures batch, my labmates and many other friends, whom I got to know here in Kanpur, who made my stay here delightful and thoroughly enjoyable.

TABLE OF CONTENTS

LIST OF TABLES

LIST OF FIGURES

ABSTRACT

Seismic response analyses in case of scenario earthquake approach or for balanced risk can be conveniently carried out if power spectral density function (PSDF) for ground acceleration is estimated with a given level of confidence in terms of known parameters like earthquake magnitude, epicentral distance, focal depth, site conditions, etc As a first step in this direction and in extension of available models for Fourier spectrum, this study proposes two empirical models for scaling PSDF of horizontal ground acceleration The first model considers earthquake magnitude, epicentral distance, focal depth, and strong motion duration as the governing parameters. The second model is based on the PSDFs normalized to 20 sec duration and a peak ground acceleration (PGA) value of $1g$, and does not consider the strong motion duration as parameter. For both models, the regression coefficients have been estimated from the PSDFs corresponding to the recorded data of western United States for three different geologic site conditions In case of each recorded time-history, the PSDF is assumed to correspond to an 'equivalent stationary' ground acceleration process which approximately gives the same expected response spectra on considering the transient transfer function as those obtained from the time-history The proposed models have been illustrated by considering three example ground motions and a parametric study has been carried out to discuss the effects of governing parameters on PSDF shapes. For crude estimation of normalized PSDFs, this study also proposes simple functional relationships for two categories of site conditions.

CHAPTER I

INTRODUCTION

1.1 General Introduction

For proper evaluation of the design seismic response of a structure in a seismic environment, it is necessary to first characterize the seismic hazard This is most commonly accomplished by the specification of (elastic) design spectrum curves for different damping ratios. These curves are usually specified in terms of an estimated peak ground acceleration (PGA) or effective peak acceleration (EPA) at the site corresponding to a 'scenario earthquake'. Considering the seismic environment of the site, this scenario earthquake is established along a nearby fault such that there is a desired level of confidence of the specified acceleration level not being exceeded in given number of years. The normalized design spectrum curves are often obtained after statistical processing of the PGA-normalized spectra corresponding to several past ground motions recorded in the similar site conditions When large data is available for a seismic environment, scaling equations may also be established (e.g , Trifunac and Anderson (1977, 1978)) and used to directly obtain more realistic estimates of design spectra. Since the scenario earthquake approach does not provide a balanced view of the seismic hazard when there are several faults near the site under consideration, balanced risk-based responses of structures have been obtained by integrating hazard models for ground motions with the random vibration-based models of structural response (see Gupta (1994), Todorovska (1994)). In the scenario earthquake as well as the balanced risk approach, it is desirable to consider the scaling

of power spectral density function (PSDF) for application to the multi-degree-of-freedom (MDOF) structures. The scaling of acceleration response spectra alone as per the conventional practice is undesirable due to the requirement of a modal combination rule. Further, by using the response spectra, it is not possible to have any information about the higher order peaks, which may play a significant role in the structural damage assessment (Basu and Gupta (1995)). The response spectra can also not be used in case of the non-classically damped systems due to the fact that the modal response in such a system is strictly not analogous to the response of a single-degree-of-freedom (SDOF) system. The use of Fourier spectra along with the response spectra accounts only for some of these problems A direct scaling of PSDF in terms of various earthquake and site parameters, say earthquake magnitude, epicentral distance, focal depth, geologic site conditions, etc., appears to be more convenient for the response analyses of variety of structural systems.

To describe a ground motion process through its PSDF, there exist various approaches as described by Gupta et al (1994). Analytical descriptions of PSDF have been suggested by idealizing the ground motion process to be (a) ideal white noise, (b) band limited white noise, or (c) filtered white noise process. Ideal white noise idealization is the simplest idealization as it corresponds to a PSDF with uniform value for all the frequencies. Band-limited white noise idealization offers more realistic improvement over this as here, the PSDF has uniform value only within a particular frequency range and is zero outside this range. The filtered white noise idealization corresponds to the PSDF proposed by Kanai (1957) and Tajimi (1960). This form of PSDF known as the Kanai-Tajimi model has been most popular with the researchers for the analytical studies.

In this model, the ground acceleration is visualized as the absolute acceleration response of a SDOF oscillator subjected to ideal white noise excitation at its base. The major advantage in this model is that a wide range of PSDFs can be described by simply varying the two parameters, i.e the ground frequency and the ground damping. Many researchers (e.g, Lai (1982), Elghadamasi et al. (1988)) have suggested the suitable values of these parameters for different soil conditions. The main drawback of this model however is that it yields a non-zero value at zero frequency which is incompatible with the finite energy in the ground motion To correct this, Clough and Penzien (1993) proposed the use of one more filter on the Kanai-Tajimi PSDF For the practical applications, however, the Fourier spectrum-based PSDFs or the response spectrum-compatible PSDFs have been more popular. Even though the earthquake ground motion is basically a nonstationary process, its strong motion component may often be treated as a weakly stationary process (Elghadamsi et al. (1988)), and the (temporal) PSDF can then be described in terms of its Fourier spectrum and duration (Gupta et al (1994)). For the motions where the initial building up portion and the decaying portion at the tail are very short compared to the total duration (as in the motions of long duration), this method yields a satisfactory description of the ground motion PSDF. As the design ground motions are commonly specified through the design (response) spectra, the response spectrum-compatible PSDFs (e.g, see Kaul (1978), Sundararajan (1980), Unruh and Kana (1981), Pfaffinger (1983) Gupta and Joshi (1993)) are often used in the practical PSDF-based applications. The concept of response spectrum-compatible PSDF is based on the idea of computing the probabilistic response spectrum from the ground motion PSDF (Udwadia and Trifunac (1974)), and on modelling the input ac-

celeration process to be an 'equivalent stationary process' Such a PSDF is computed by an iterative scheme, so as to match the expected peak responses of a set of SDOF oscillators with the given response spectrum ordinates. In various schemes proposed on this basis, it has been found that the PSDF curves obtained from response spectra for different damping ratios are substantially different from each other. This is due to the basic assumption in these methods that the response of a dynamical system to a stationary process is a stationary process. However, it has been shown by Caughey and Stumpf (1961) that, apart from the inherent nonstationarity in the ground motion, additional nonstationarity is introduced into the response process due to the finite operating time of excitation. The method proposed by Shrikhande and Gupta (1996) explicitly takes care of this additional nonstationarity by the use of transient transfer function. In this method, the earthquake ground motion process is modelled as a finite duration segment of a stationary random process such that this is equivalent to the given nonstationary process in terms of the largest peak responses of a set of SDOF oscillators This method is more realistic in the sense that it is independent of the system characteristics and thus similar PSDFs are obtained for the spectra for different damping ratios yielding a more consistent description of the ground motion. Evolutionary PSDF corresponding to an amplitude-modulated stationary process (e.g., see Shinozuka (1970), Liu (1970), Lin and Yong (1987)) explicitly accounts for the nonstationarity in the ground motion process through the use of a time-dependent envelope function Based on this model, Spanos and Vargas Loli (1985) have suggested the computation of spectrum-compatible evolutionary PSDF. However, this model is not accurate enough due to ignoring the frequency nonstationarity in the ground motion, and is not as simple and

elegant as the model of equivalent stationary process

Except for the availability of a few empirical forms of design PSDF in the recent years (Chang et al (1991)), no attempt has been made yet to establish an empirical relation to scale the ground PSDF in terms of the earthquake parameters like epicentral distance, magnitude, geologic site condition, focal depth etc A substantial amount of work has however been done to develop scaling relationships for other functionals like PGA, Fourier spectrum, pseudo spectral velocity (PSV), and spectral acceleration (SA). Scaling relations for PGA in terms of magnitude and epicentral distance have been proposed by several researchers (for example, see Gutenberg and Richter (1942, 1956), Neumann (1954), Housner (1965), Blume (1965), Kanai (1966), Milne and Davenport (1969), Esteva (1970), Cloud and Perez (1971), Schnabel and Seed (1973)). Each of these correlations was obtained by fitting an attenuation curve to a limited number of data points. Later, Trifunac and Brady (1976) used the Richter attenuation function (Richter (1958)) to correlate the means and standard deviations of the peaks of ground acceleration, velocity and displacement with magnitude for different site conditions The Richter attenuation function was obtained empirically from the data for Southern California, and this thus contained an 'average' information about the properties of wave propagation regarding geometric spreading, scattering, etc through the crust in Southern California Trifunac (1976a) later improved this model by attaching appropriate confidence levels to the predicted peak amplitudes and by considering magnitude, site condition, epicentral distance as the scaling parameters in the equation By obtaining independent estimates (based on source mechanism theory) of the peaks of acceleration, velocity and displacement and by comparing

those with the estimates of the proposed scaling relationship, Trifunac (1976a) observed that the attenuation law of Trifunac and Brady (1976) could be extrapolated to give satisfactory results for distances less than 20 km also The model of Trifunac (1976a) was later generalized to other spectral quantities, e g , to Fourier spectra by Trifunac (1976b), to absolute acceleration spectra by Trifunac and Anderson (1977), and to pseudo relative velocity spectra by Trifunac and Anderson (1978) at a set of discrete periods These models facilitated the direct description of design ground motion in terms of the known parameters at a desired confidence level.

The attenuation function used by Trifunac and Brady (1976) had the limitation that it was independent of parameters like magnitude (which effectively represented the source dimension of an earthquake), focal depth and geological environment of the site. In the early 80's, as more strong motion data from Northern and Southern California became available, it was attempted to model the attenuation in a better way by incorporating the fact that the high-frequency waves attenuate much faster compared to the low frequency waves. Trifunac and Lee (1985a) suggested a frequency-dependent attenuation function which was composed of two parts, one depending on the frequency, i.e the attenuation coefficient, and the other depending on the source-to-station representative distance. The 'representative distance' as proposed by Gusev (1983) varies as a function of the earthquake magnitude, and thus incorporating this in the attenuation function represented an improvement over the Richter model. The new attenuation function was first employed for the scaling of Fourier amplitude spectrum by Trifunac and Lee (1985b), and later in several other scaling studies (e.g , see Trifunac and Lee (1985c), Trifunac (1987), Lee (1987)).

In various scaling equations presented in the past 20 years (e g , see Trifunac (1976a, 1976b), Trifunac and Anderson (1977), Trifunac and Lee (1978, 1979, 1985b, 1985c)), the rate of growth of spectral amplitudes with earthquake magnitude has been considered to be linear up to a certain minimum value of the magnitude Beyond this range and up to a certain maximum value, the growth is assumed to have a parabolic form The spectral amplitudes are considered to be invariant of the magnitudes higher than this maximum value. Though this functional form of the growth lacked any physical justification, it was supported by the observed trend of data (Trifunac (1976a, 1976b), Trifunac and Brady (1976)).

It is well known that the various ground motion functionals have strong dependence on the geologic and soil conditions at the site. In some of the works reported (e g., those by Trifunac (1976b), Trifunac and Anderson (1977), Trifunac and Lee (1985b, 1985c)), the site classification was based on the geological characteristics in terms of the hardness of the soil surrounding the recording stations This classification was proposed by Trifunac and Brady (1976), and the main advantage of using such a classification is that this information is available from the knowledge of surface geology only. However, in this classification, the 'geometric characteristics' (i.e., the horizontal and vertical extent of the local inhomogeneities) regarding the local soil conditions are overlooked To overcome this drawback, the recording site condition was described through the depth of sediments beneath the recording station (Trifunac and Lee (1978)). The idea behind this basis of site classification was that the wave velocity, material rigidity and density increase substantially in going with depth from sediments to rock Later, in a further improvement, the parameter of local soil conditions as defined by Seed et al (1976) was considered simultaneously with the geological site

conditions by Trifunac (1987) and Lee (1987)

It is apparent from the above that more and more parameters were included in the scaling relations with the passage of time for narrowing down the scatter of data points. Further, in this direction, Lee et al. (1995) has recently presented scaling relations for peak ground acceleration, velocity and displacement by explicitly including the effect of the transmission path

Along with the magnitude-based scaling relationships as discussed above, relationships incorporating earthquake intensity, e g , Modified Mercalli Intensity (MMI), as a parameter have also been developed for different spectral quantities In spite of having inherent drawbacks, e.g , large uncertainty in the intensity data, these relationships have been developed because in many seismic regions of the world, no measurements of the strong ground motions are available Many historical records are in fact based on locally developed intensity scales only The intensity-based scaling relationships were first proposed for scaling peak ground acceleration (for example, see Ishimoto (1932), Kawasumi (1951), Hershberger (1956), Richter (1958), Neumann (1954), Medvedev and Sponheuer (1969), Okamoto (1973), Savarensky and Kirnos (1955), Trifunac and Brady (1975a)). Later, scaling relationships were also developed for other functionals, e.g , by Trifunac (1979) for absolute acceleration spectra, by Trifunac and Anderson (1978), Trifunac and Lee (1985b), and Trifunac (1987) for Fourier spectrum, and by Trifunac and Lee (1978), Trifunac and Lee (1985c), and Lee (1987) for PSV.

As mentioned earlier, more refined scaling relationships with greater number of parameters have been able to describe the ground motion functionals

more accurately as has been indicated by the gradual narrowing down of the spread of the spectral amplitude over a given confidence interval It is expected that with further increase in the size of the database, further refinements will be proposed in the scaling models involving perhaps more number of parameters like transmission path, stress drop, seismic moment, etc. However, due to the practical constraints, all of these parameters may not always be available to the designer in seismic hazard quantification Keeping this in view and for simplicity in the first step towards developing a scaling model of PSDF, the scaling model as proposed by Trifunac and Lee (1985b) for Fourier spectrum amplitudes has been considered as the basis in this study This model makes use of those parameters which are routinely employed to describe the overall size and severity of the earthquake, namely, epicentral distance, magnitude, focal depth, and geologic site condition Further a model for the Fourier spectrum amplitudes has been considered as the basis due to the direct dependence of temporal PSDF of a ground motion record on its Fourier spectrum amplitudes and strong motion duration (see, for example, Bendat and Piersol (1986))

Two scaling models have been presented in this study. Both models consider epicentral distance, magnitude, focal depth, and site geology as the governing parameters. In addition to these, the strong motion duration has also been considered as a parameter in case of the first model. Since there is no standard and well accepted definition of strong ground duration, though several definitions have been proposed in the past two decades, e g , those by Bolt (1973), Page et al (1972), Trifunac and Brady (1975b), McCann and Shah (1979), Kawashima and Aizawa (1989), Vanmarcke and Lai (1980), Mohraz and Peng (1989), and Trifunac and Westermo (1982), the second model has been proposed for 'normal-

ized' PSDF to a fixed duration of 20 sec The PSDF data used for the second model is also normalized to a fixed value of expected PGA, besides normalization to the same duration, since it is common to characterize the severity of design ground motions by PGA values The PSDF data has been generated from the response spectra of the recorded motions by using the spectrum-compatible PSDF definition of Shrikhande and Gupta (1996) Both of the proposed models do not consider the site geology as a parameter Instead, the scaling coefficients have been regressed separately for three different (geologic) site conditions Also, both models have been proposed for the horizontal component of ground motion only, and thus, the parameter of component direction also has not been considered. With a view to further simplify the model for normalized PSDF for crude applications, simple average shapes have also been estimated for normalized PSDF on the same lines as in Seed et al. (1976) for PGA-normalized response spectra The database used for the present study consists of the 494 'free-field' records of 106 earthquakes in Western United States, starting from 1931 Long Beach Earthquake, California to the 1984 Morgan Hill Earthquake, California, as in Lee and Trifunac (1987)

1.2 Organization

This work has been presented in three chapters following this chapter

In Chapter II, the first scaling model, correlating the horizontal ground PSDF with earthquake magnitude, epicentral distance, focal depth and duration, has been presented for different site conditions. Least square estimates for various period-dependent coefficients have been obtained by regression analysis and

the deviations of the actual PSDF values from the estimated values have been described probabilistically The proposed model has been illustrated by comparing the PSDFs of a few example recorded motions with their probabilistic estimates as obtained from the proposed model, and by presenting the estimated PSDFs with 50% level of confidence for varying durations, magnitudes, epicentral distances and site conditions

In Chapter III, the second scaling relationship and the 'average' PSDFs based on the 'normalized' PSDF data have been presented As in Chapter II, the second scaling relationship has also been illustrated through comparison of actual PSDFs with the probabilistic estimates of PSDFs and through a parametric study Further, simple functional forms have been suggested for the average PSDFs in different site conditions

A brief summary and conclusions of this study have been presented in Chapter IV.

CHAPTER II

SCALING OF PSDF IN TERMS OF EARTHQUAKE MAGNITUDE, EPICENTRAL DISTANCE, FOCAL DEPTH AND STRONG MOTION DURATION

2.1 Brief Overview

In this chapter, a new regression model has been proposed for scaling the PSDF of the horizontal component of ground motion process. This assumes the parametric dependence of PSDF on earthquake magnitude, epicentral distance, focal depth, strong motion duration and site geology. The proposed model is a simple extension of the model proposed by Trifunac and Lee (1985b) for the scaling of Fourier spectrum amplitudes. The PSDF corresponding to a recorded ground motion has been estimated from the response spectra of this motion by using the procedure suggested by Shrikhande and Gupta (1996) The scaling coefficients have been determined from the PSDFs corresponding to a data-set of 988 recorded ground motions for three different geological site conditions. These ground motions have been recorded during the 106 earthquake events in the Western U.S.A region till 1984. In order to use the regressed coefficients for estimating PSDF at a given confidence level, the inherent variations in the recorded PSDF values have been probabilistically modelled at different periods.

2.2 Scaling Relationship

In the absence of any previous study on the scaling of PSDFs, a scaling

relationship consistent with the following relationship between Fourier spectrum, $FS(T)$, and PSDF, $PSDF(T)$, has been considered According to this, the (temporal) PSDF of the ground motion at period, T, may be estimated as (e g., see Bendat and Piersol (1986))

$$PSDF(T) = \frac{|FS(T)|^2}{\pi T_s} \tag{2.1}$$

where, T_s is the strong motion duration of the ground motion. On considering the preliminary scaling model for Fourier spectrum as presented by Trifunac and Lee (1985b), the scaling equation for PSDF of the horizontal ground motion may be assumed to be

$$\log_{10} PSDF(T) = 2M + 2Att(\Delta, M, T) + b_1(T)M + b_2(T)\Delta + b_3(T) + b_4(T)M^2 + b_5(T)\log_{10} T_s \,. \tag{2.2}$$

More sophisticated models for scaling of the Fourier spectrum amplitudes also consider a parameter for the local site conditions (Trifunac (1987)). However, this model has been chosen in order to obtain a preliminary scaling relationship which uses only the readily available earthquake paramaters. In Eq (2.2), $b_i(T)$'s are the period-dependent coefficients and M is the 'published' magnitude. A 'published' magnitude corresponds to the local magnitude if $M \leq 6.5$ and to the surface wave magnitude if $M > 6.5$ (Trifunac and Lee (1985a)). Further, Δ is the 'representative distance' which basically represents the effective source-to-station distance It has been defined by Gusev (1983) in terms of the epicentral distance, R, the focal depth, H, the size of the fault, S, and the coherence radius, S_0, of the source function as

$$\Delta = S\left(\ln \frac{R^2 + H^2 + S^2}{R^2 + H^2 + {S_0}^2}\right)^{-\frac{1}{2}} \,. \tag{2 3}$$

The coherence radius, S_0, is period-dependent and it can be approximated as $\beta T/2$ where β is the velocity of radiation of waves having period, T (Trifunac and Lee (1985a)). β has been assumed to be 1000 m/sec in this study The term, $\mathcal{A}tt(\Delta, M, T)$ is the period-dependent attenuation function proposed by Trifunac and Lee (1985a) as

$$\begin{aligned} \mathcal{A}tt(\Delta, M, T) &= \mathcal{A}_0(T) \log_{10} \Delta && R \leq R_0 \\ &= \mathcal{A}_0(T) \log_{10} \Delta_0 - (R - R_0)/200 && R > R_0 \ , \end{aligned} \tag{2.4}$$

where R_0 is the transition distance from the earthquake source at which the surface waves start dominating the ground motion, and Δ_0 is the representative distance corresponding to R_0 Further, $\mathcal{A}_0(T)$ is the empirically determined attenuation function at time period, T, and is represented as (Trifunac and Lee (1985a))

$$\begin{aligned} \mathcal{A}_0(T) &= -0.767079 + 0.271556 \log_{10} T - 0\ 52564\ (\log_{10} T)^2 \ ; \quad T < 1.8 \text{ sec} \\ &= -0.732025 \qquad\qquad\qquad\qquad\qquad\qquad\qquad\qquad ; \quad T \geq 1.8 \text{ sec} \ . \end{aligned} \tag{2.5}$$

As the values of the fault size are usually not available, an empirical relationship has been proposed by Trifunac and Lee (1985a) to estimate this from the earthquake magnitude at each period as

$$S = 0.2 + \frac{(M-3)}{3.5}(S_{6.5} - 0\ 2) \ , \tag{2.6}$$

where $S_{6\,5}$ is the fault size for $M = 6.5$. Its value for six different period ranges has been obtained by Trifunac and Lee (1985a) through iterative calculations, and those values have been adopted for the present study.

It may be noted that the present study considers the horizontal ground motions only. Hence, the parameter, v which has been used by Trifunac and Lee (1985b) for the component direction of motion has been omitted The proposed model also considers the effect of geologic site conditions in a different manner. Instead of considering s as a parameter in regression analysis, with $s = 0$, 1, 2 representing respectively the alluvium, intermediate and hard rock conditions, three separate regression analyses have been carried out for these site conditions. Thus, instead of single scaling equation with s included as a parameter, three different scaling equations have been developed in this study for the three different site conditions It may also be noted that the new scaling parameter, T_s, does not have a unique or well-accepted definition since the earthquake ground motions are highly non-stationary and T_s is deemed to refer to the strong motion part of an earthquake ground motion. For the present study, the definition by Trifunac and Brady (1975b) has been adopted since the strong motion duration according to this definition can be derived from a recorded accelerogram by considering the arrival of seismic energy with time in a very simple manner. Due to this reason, this definition has been widely used in several studies over the past two decades. By this definition, the continuous time interval in which the most significant contribution to the seismic energy takes place is considered to be the 'strong motion duration'. The seismic energy at a time instant, $t = t'$, is measured by the integral of square of acceleration from $t = 0$ to $t = t'$, and the strong motion duration is defined as the difference of those time instants at which this integral attains 5% and 95% of the total seismic energy (measured at the end of the record).

2.3 Raw PSDF Data and Data Selection

The present study is based on the EQINFOS data bank (Lee and Trifunac (1987)). This consists of 988 records for horizontal component of ground motion from 106 earthquakes which were recorded from 1931 Long Beach Earthquake, California to the 1984 Morgan Hill Earthquake, in the Western U.S.A region Some of these records have been left out of the present regression analysis due to the lack of complete details. For example, no reliable estimates of earthquake magnitude were available for AU294, AU295, AU297, AU298 records. For the event # 7, 10, 11, 12, 25, 34, 35, 38 and for record # 1341 and 1381, the recorded time histories were incomplete. For some of the records, namely BA142, AB025, AU295, AU297, AB032, AB029, AB028, AU310, BA144, BA255, AY372, no information about the geologic environment of the site was available. Thus, this study has been based on 960 recorded accelerograms, 733 for alluvium site conditions, 85 for intermediate site conditions and 142 for hard rock site conditions For a few early records, the focal depth, H, values of the earthquakes were not available. In such cases, H has been uniformly assumed to be 16.0 km (Trifunac and Brady (1975a)).

For evaluating PSDF corresponding to each accelerogram record prior to the regression analysis, the method of computing spectrum-compatible PSDF as proposed by Shrikhande and Gupta (1996) has been employed with the duration taken to be the same as the strong motion duration of the record. Three smoothed response spectrum curves corresponding to 0.01, 0.02 and 0.05 damping ratios have been considered in case of each record, and these spectra have been assumed to be the 'expected' spectra for the underlying ground acceleration

process In each of the three cases, the matching of the computed spectrum with the target spectrum has been achieved within 1 5% of the average error at 91 periods between 0.04 and 15.0 sec. The three PSDFs obtained from the three response spectra have been then averaged out to give the mean information about the PSDF of the underlying process. Let this be denoted by $PSDF(T)$.

Since the number of records for different magnitude classes, namely 3 0–3.9, 4 0–4.9,. ., 7.0–7.9, were substantially different from one another, and for some of the earthquakes (for example, 1971 San Fernando Earthquake), there were excessive number of records which could have a bias on the final coefficient values, data screening has been carried out. To accomplish this, a technique as reported in the previous works on regression analyses (e g , see Trifunac (1976b), Trifunac and Anderson (1977, 1978), Trifunac and Lee (1978, 1985b, 1985c)) has been employed. For each of the site categories (i.e , alluvium, intermediate and hard rock site), all the PSDF data has been partitioned into 5 groups corresponding to the different magnitude classes. Further, to properly balance the effects of attenuation at small and large distances, the data in each of the above groups has been sub-divided into two sub-groups, one for $R \leq 100$ km and the other for $R > 100$ km. Various PSDF data points in each of these sub-groups have been then rearranged at a period, T, in such a fashion that the value, $(\log_{10} PSDF(T) - 2M - 2Att(\Delta, M, T))$ decreased monotonically. Since the objective of the data selection procedure is to ensure that approximately same number of data points represent each of the sub-groups, different values of confidence level, say p, have been chosen and the data points in a sub-group which correspond to those levels only have been considered Thus, if m levels of probability, $p = p_1, p_2,..., p_m$, are specified and if $k_1, k_2,..., k_m$ denote the nearest

integers to $p_1 n$, $p_2 n$, ., $p_m n$ respectively, the k_1th, k_2th, .., k_mth data points in a sub-group of n data points have been considered Thus, in case of the sub-groups corresponding to $R \leq 100$ km, the chosen p values are $p_1 = 0\ 05$, $p_2 = 0.10$, , $p_m = 0\ 95$ with $m = 19$ In some of these sub-groups, if n is less than 19, all the data points have been taken into account For the sub-groups corresponding to $R > 100$ km, fewer records were available, and hence, a maximum of 5 points only have been selected in each sub-group (with $p_1 = 0\ 1667$, $p_2 = 0\ 3333$,..., $p_5 = 0\ 8333$) It may be mentioned here that the above selection process screens out different sets of data points at different periods, and thus, all the available PSDF data is effectively utilized in the regression

2.4 Regression Analysis and Distribution of PSDF

Linear regression analyses have been carried out on 733 PSDFs for alluvium site conditions, 85 PSDFs for intermediate site conditions and on 142 PSDFs for hard rock sites at 91 values of T, ranging from 0 04 to 15.0 sec. In case of each of these site conditions, let the least square estimates of the coefficients, $b_1(T)$, $b_2(T)$, $b_3(T)$, $b_4(T)$ and $b_5(T)$, as obtained from the regression analysis at each period, T, be denoted by $\hat{b}_1(T)$, $\hat{b}_2(T)$, $\hat{b}_3(T)$, $\hat{b}_4(T)$ and $\hat{b}_5(T)$ respectively. The 95% confidence intervals of these coefficients have been estimated by assuming those to be distributed as per the student's t-distribution with $(n-5)$ degrees of freedom where n is the total number of data points used for regression. The variance of each of the coefficients has been computed for this purpose as in Westermo and Trifunac (1978). The least square as well as the 95% confidence estimates for each coefficient have been smoothed along the $\log_{10} T$ axis

On substituting the (smoothed) values of the coefficients, $\hat{b}$'s, in Eq. (2.2), we obtain the least square estimate of $PSDF(T)$ as

$$\log_{10} \widehat{PSDF}(T) = 2M + 2\mathcal{A}tt(\Delta, M, T) + \hat{b}_1(T)M + \hat{b}_2(T)\Delta + \hat{b}_3(T) + \hat{b}_4(T)M^2 + \hat{b}_5(T)\log_{10} T_s \ . \tag{2.7}$$

For a given set of values of T, M, Δ and T_s, $\log_{10} \widehat{PSDF}(T)$ represents a parabolic variation in M This parabolic dependence on M has been however found to be valid, in case of Fourier spectrum amplitudes, only within a particular interval of magnitude (Trifunac (1976a)). In fact, for the small magnitudes, the growth of logarithm of Fourier spectrum has been found to be proportional to the magnitude, and for higher values of M, this has been found to be invariant of M (Trifunac (1976a)) To model this behaviour in a simple manner, it has been assumed in view of Eq (2 1) that the growth rate of $\log_{10} \widehat{PSDF}(T)$ with M corresponds to a slope equal to 2 for $M < M_{min}$. For $M_{min} \leq M \leq M_{max}$, this slope decreases gradually and finally becomes zero for $M > M_{max}$. It may be noted that this assumption is based on neglecting the variations in strong motion duration with magnitude in these ranges. Thus, Eq. (2.7) has been considered to be valid only in the range, $M_{min} \leq M \leq M_{max}$, where

$$M_{min} = -\frac{\hat{b}_1(T)}{2\hat{b}_4(T)} \ , \tag{2.8}$$

$$\text{and} \quad M_{max} = -\frac{2 + \hat{b}_1(T)}{2\hat{b}_4(T)} \ . \tag{2.9}$$

Eq. (2 7) is then modified to

$$\log_{10}\widehat{PSDF}(T) = 2Att(\Delta, M, T) + \begin{cases} 2M + \hat{b}_1(T)M_{\min} + \hat{b}_2(T)\Delta + \hat{b}_3(T) \\ \quad + \hat{b}_4(T)M_{\min}^2 + \hat{b}_5(T)\log_{10}T_s\,; & M \le M_{\min} \\ 2M + \hat{b}_1(T)M + \hat{b}_2(T)\Delta + \hat{b}_3(T) \\ \quad + \hat{b}_4(T)M^2 + \hat{b}_5(T)\log_{10}T_s\,, & M_{\min} \le M \le M_{\max} \\ 2M_{\max} + \hat{b}_1(T)M_{\max} + \hat{b}_2(T)\Delta + \hat{b}_3(T) \\ \quad + \hat{b}_4(T)M_{max}^2 + \hat{b}_5(T)\log_{10}T_s\,; & M_{\max} \le M \end{cases} \tag{2.10}$$

and the corresponding residual describing the deviation of the recorded PSDF from the estimated PSDF at period, T, is given by

$$\varepsilon(T) = \log_{10} PSDF(T) - \log_{10}\widehat{PSDF}(T)\,. \tag{2.11}$$

At a fixed T, all the residuals have been computed from the raw PSDF data for each of the soil conditions by using this equation, and the actual probability distribution, $p^*(\varepsilon, T)$ has been obtained from the fraction of residuals. According to this, the probability that a chosen value of $\varepsilon(T)$ will not be exceeded has been evaluated simply by finding out the ratio of the number of residual values less than the chosen $\varepsilon(T)$ to the total number of residual data values. It is assumed that a normal distribution function with the mean, $\mu(T)$, standard deviation, $\sigma(T)$, and described as

$$p(\varepsilon, T) = \frac{1}{\sigma(T)\sqrt{2\pi}} \int_{-\infty}^{\varepsilon(T)} \exp\left[-\frac{1}{2}\left(\frac{x - \mu(T)}{\sigma(T)}\right)^2\right] dx \tag{2.12}$$

closely approximates the computed distribution, $p^*(\varepsilon, T)$. Hence, the values of mean and standard deviation, say $\hat{\mu}(T)$ and $\hat{\sigma}(T)$ respectively, which provide the best fit of Eq. (2.12) with $p^*(\varepsilon, T)$ have been estimated. These least square estimates, $\hat{\mu}(T)$ and $\hat{\sigma}(T)$, have been then smoothed along $\log_{10}T$ axis for each of the soil conditions. The smoothed values, $\hat{\mu}(T)$ and $\hat{\sigma}(T)$, now form the basis for

estimating the PSDF with a desired level of confidence. At a period T, Eq (2.12) can be used to estimate $\varepsilon(T)$ corresponding to a given level of confidence and be added to the calculated $\widehat{PSDF}(T)$ (see Eq (2.10)) for this purpose. To check the reliability of the assumption that the residuals are normally distributed, two statistical 'goodness of fit' tests, namely the chi-square test and the Kolmogorov-Smirnov (KS) test, have been conducted. The KS statistics, $KS(T)$ and the chi-square statistics, $\chi^2(T)$ have been calculated at each of the 91 periods for different site conditions, and have been compared with the respective 95% cut-off values.

2.5 Results and Discussion

The smoothed least square estimates, $\hat{b}_1(T)$ through $\hat{b}_5(T)$, and the 95% confidence estimates of the regression coefficients are shown in Figs. 2.1(a) to 2.1(c) for alluvium site ($s = 0$), intermediate site ($s = 1$) and hard rock site ($s = 2$) conditions respectively. The least square estimates are shown by the solid lines while the 95% confidence estimates are shown by the dashed lines. Tables 2.1(a) to 2.1(c) present the (smoothed) least square estimates, $\hat{b}_1(T)$ through $\hat{b}_5(T)$, and the (smoothed) values of $\hat{\mu}(T)$, $\hat{\sigma}(T)$ at 12 selected periods for the three site conditions.

Figs. 2.2(a) to 2.2(c) show the comparison of the actual residuals with the estimated residuals (corresponding to the smoothed $\hat{\mu}(T)$ and $\hat{\sigma}(T)$ values in Eq. (2.12)) for the alluvium site, intermediate site, and hard rock conditions respectively. In each figure, the solid lines represent the actual residuals for $p^* = 0.1$, 0.3, 0.5, 0.7 and 0.9 while the dashed lines represent the estimated residuals for $p = 0.1$, 0.3, 0.5, 0.7 and 0.9. It may be observed that the estimated

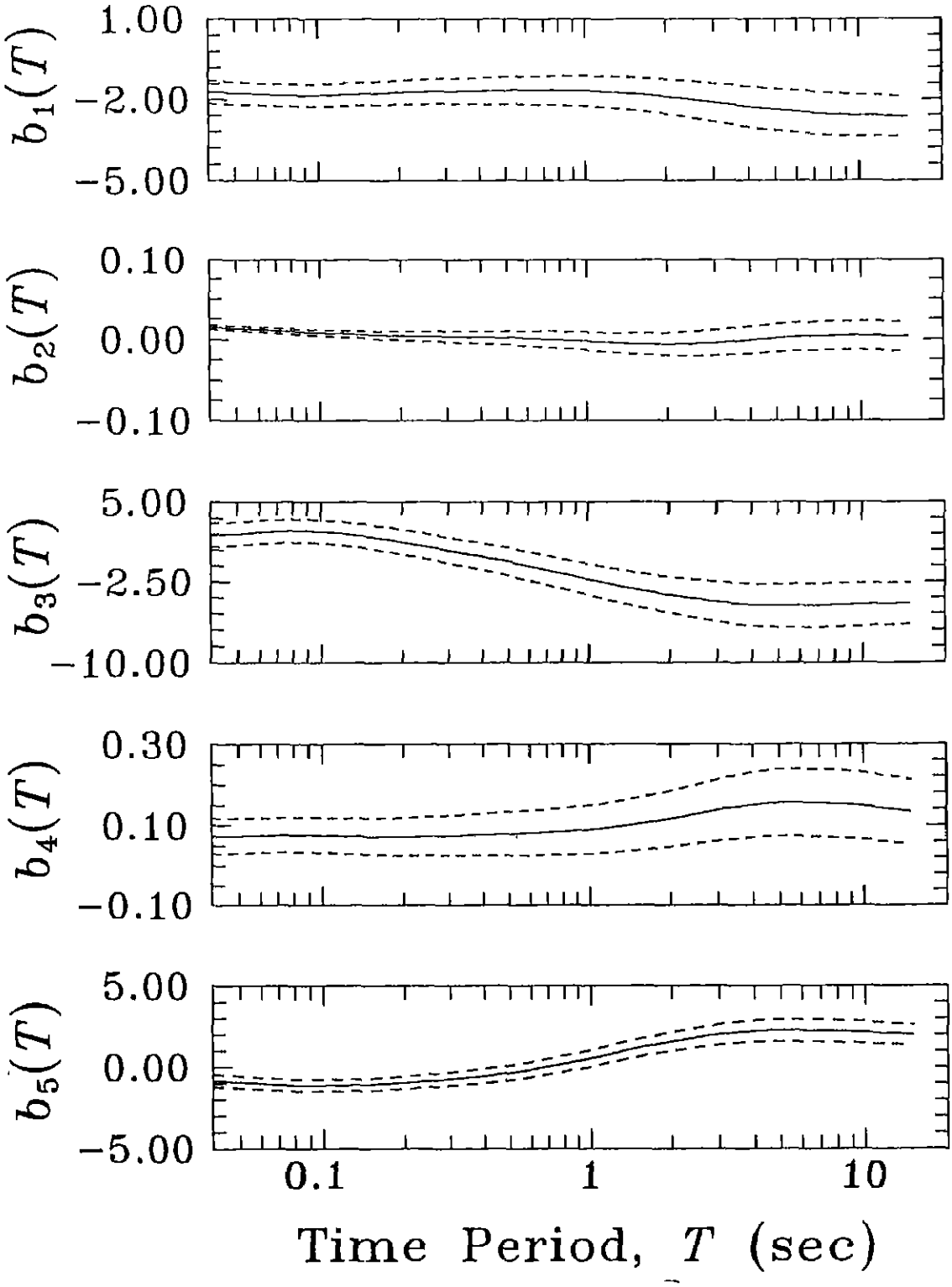

Figure 2.1(a) Regression Coefficients for Alluvium Site Condition.

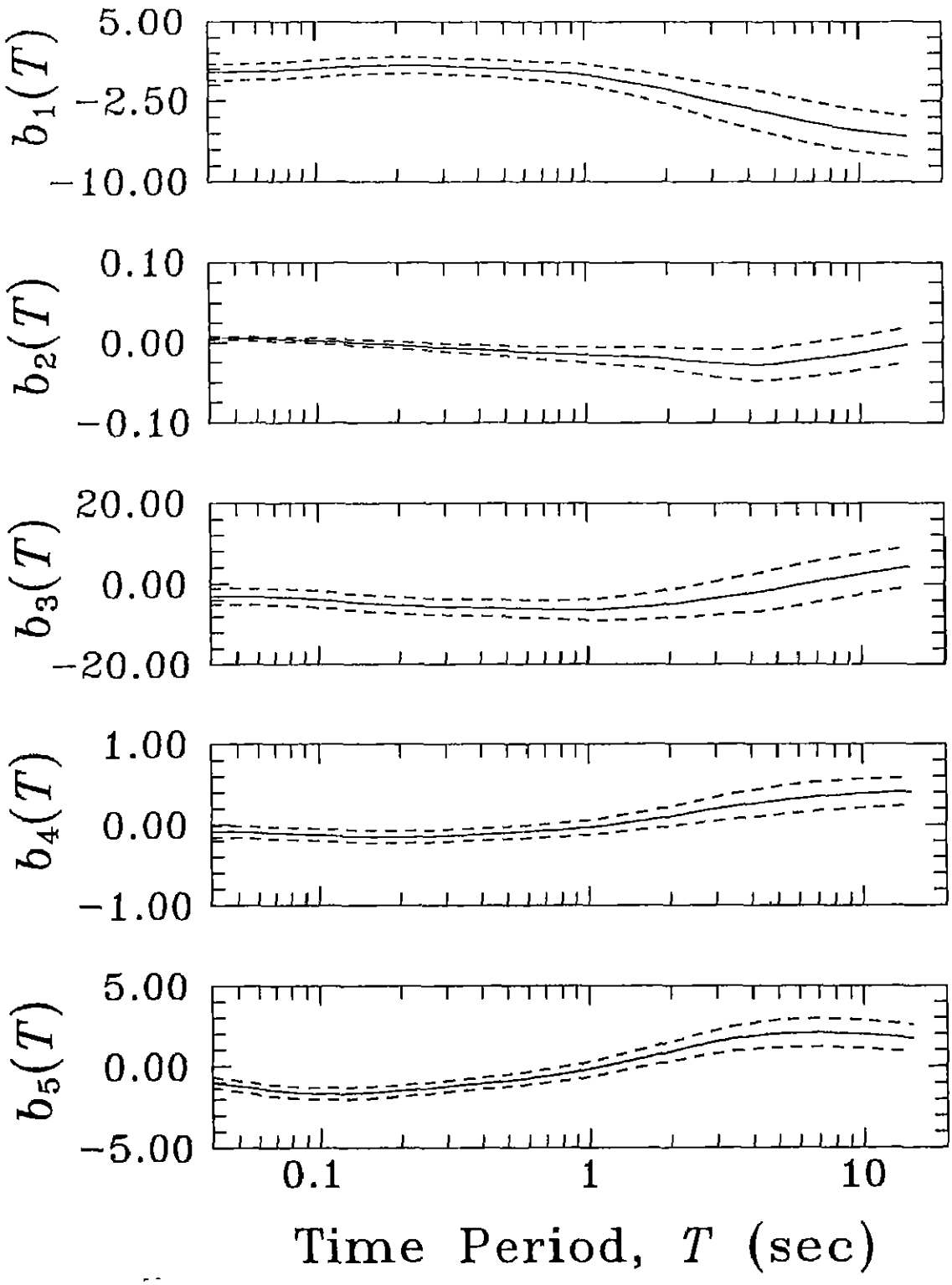

Figure 2.1(b) Regression Coefficients for Intermediate Alluvium Site Condition.

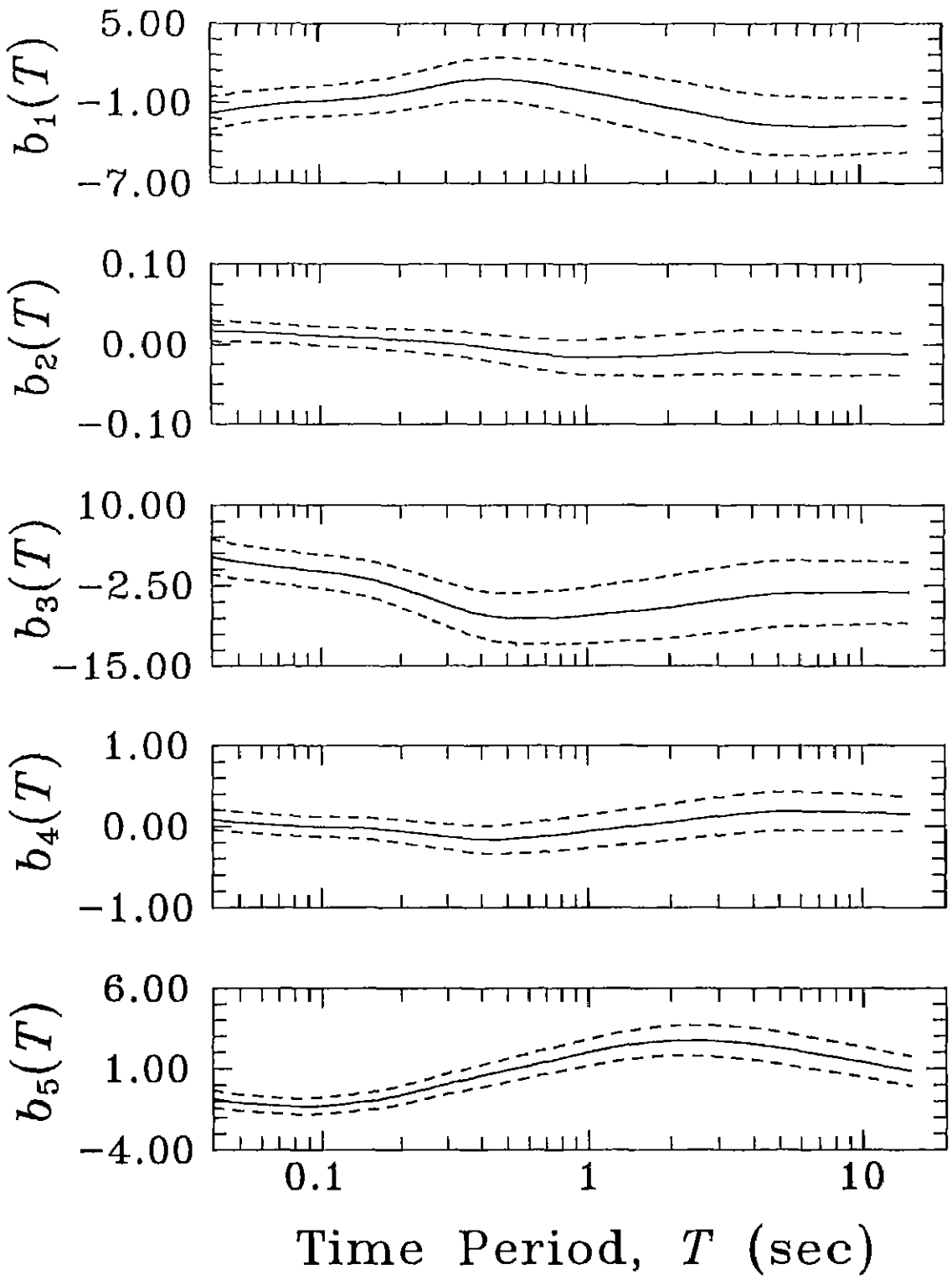

Figure 2.1(c) Regression Coefficients for Hard Rock Site Condition.

Table 2.1(a) - Least Square Estimates of Regression Coefficients and Residual Parameters for Alluvium Site Condition

Period, T (sec)	Least Square Estimates of Regression Coefficients					Residual Parameters	
	$\hat{b}_1(T)$	$100\hat{b}_2(T)$	$\hat{b}_3(T)$	$10\hat{b}_4(T)$	$\hat{b}_5(T)$	$\hat{\mu}(T)$	$\hat{\sigma}(T)$
0.04	-1.720	1.480	1.910	0.735	-0.811	0.109	0.673
0.065	-1.830	1.100	2.220	0.757	-1.050	0.104	0.650
0.11	-1.840	0.725	2.150	0.749	-1.130	0.109	0.640
0.19	-1.750	0.435	1.370	0.724	-0.974	0.117	0.638
0.34	-1.690	0.274	0.224	0.762	-0.653	0.120	0.663
0.50	-1.680	0.175	-0.590	0.797	-0.353	0.121	0.707
0.90	-1.680	-0.175	-2.020	0.871	0.376	0.136	0.822
1.60	-1.810	-0.560	-3.330	1.060	1.260	0.167	0.979
2.80	-2.080	-0.464	-4.260	1.340	1.940	0.199	1.213
4.40	-2.330	0.013	-4.710	1.540	2.250	0.189	1.443
7.50	-2.540	0.444	-4.700	1.540	2.230	0.075	1.583
14.00	-2.640	0.379	-4.530	1.360	2.040	-0.101	1.517

Table 2.1(b) - Least Square Estimates of Regression Coefficients and Residual Parameters for Intermediate Site Condition

Period,	Least Square Estimates of Regression Coefficients					Residual Parameters	
T (sec)	$\hat{b}_1(T)$	$100\hat{b}_2(T)$	$\hat{b}_3(T)$	$10\hat{b}_4(T)$	$\hat{b}_5(T)$	$\hat{\mu}(T)$	$\hat{\sigma}(T)$
0.04	0 179	0 590	-3 050	-0 832	-0 971	-0 015	0 395
0 065	0 257	0 442	-3 130	-0 991	-1.430	-0 007	0 418
0 11	0.575	0.156	-3 960	-1 310	-1 650	-0 007	0 437
0 19	0 845	-0 280	-5 130	-1.510	-1 500	-0.011	0.441
0.34	0 708	-0 759	-5 710	-1.280	-1.130	-0.011	0 450
0 50	0 492	-1 060	-5 900	-1 000	-0.856	-0.013	0 477
0.90	0 078	-1.510	-6 310	-0.482	-0.312	-0.020	0 564
1.60	-0 923	-1.800	-5.550	0.534	0 541	-0.021	0.699
2 80	-2 310	-2.480	-3 650	1.860	1 430	-0.020	0.902
4.40	-3 420	-2.800	-1 780	2.820	1 950	-0.040	1.094
7.50	-4.690	-1.940	1 110	3 640	2.060	-0 129	1.257
14.00	-5.710	-0 529	3.930	4.080	1 790	-0.302	1.291

Table 2 1(c) - Least Square Estimates of Regression Coefficients and Residual Parameters for Hard Rock Site Condition

Period,	Least Square Estimates of Regression Coefficients					Residual Parameters	
T (sec)	$\hat{b}_1(T)$	$100\hat{b}_2(T)$	$\hat{b}_3(T)$	$10\hat{b}_4(T)$	$\hat{b}_5(T)$	$\hat{\mu}(T)$	$\hat{\sigma}(T)$
0 04	-1 850	1 730	2 030	0 911	-0.836	-0 015	0 651
0 065	-1.200	1.410	0 526	0 233	-1 240	-0.042	0 664
0 11	-0 882	1 000	-0 540	-0 073	-1 210	-0 051	0.688
0 19	-0.398	0 622	-2 530	-0 527	-0 682	-0.055	0.750
0.34	0 550	0.000	-6 110	-1 450	0 298	-0.063	0.859
0 50	0.718	-0.696	-7 450	-1 560	0.898	-0 071	0.957
0.90	0 006	-1.600	-7 210	-0.785	1 840	-0.089	1.148
1 60	-0 991	-1 510	-6 230	0.192	2 600	-0.109	1 342
2.80	-1.960	-1.100	-4 930	1 140	2 720	-0 146	1 509
4.40	-2.630	-0.961	-3.840	1 810	2 420	-0 208	1 615
7.50	-2 780	-1.150	-3.560	1.840	1 790	-0.356	1.666
14.00	-2 710	-1 220	-3.550	1.590	0 960	-0.572	1.706

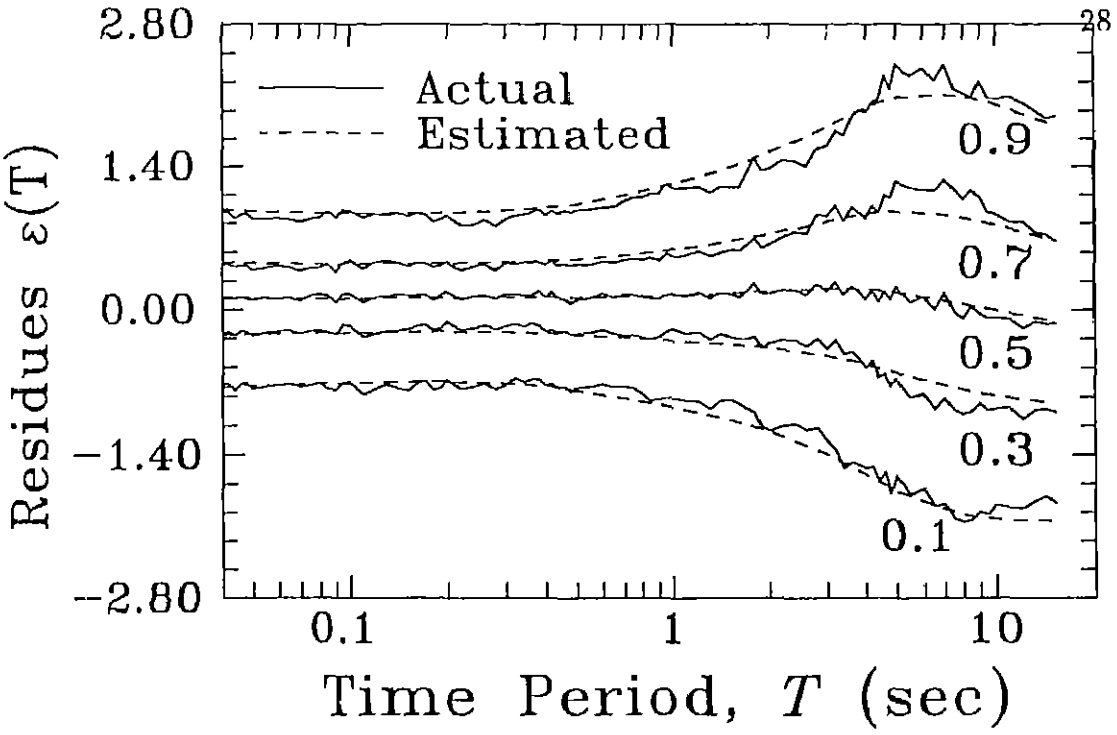

Figure 2.2(a) Residuals for p, $p^* = 0.1$, 0.3, 0.5, 0.7 and 0.9 in Case of Alluvium Site Condition.

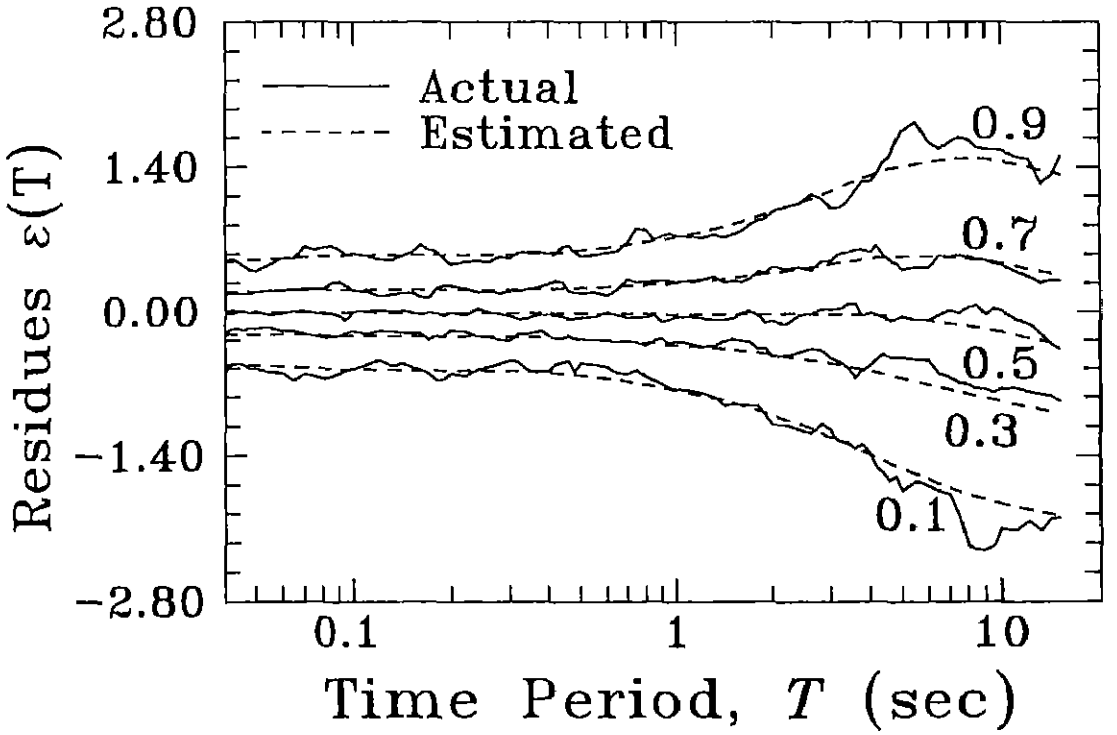

Figure 2.2(b) Residuals for p, $p^* = 0.1$, 0.3, 0.5, 0.7 and 0.9 in Case of Intermediate Site Condition.

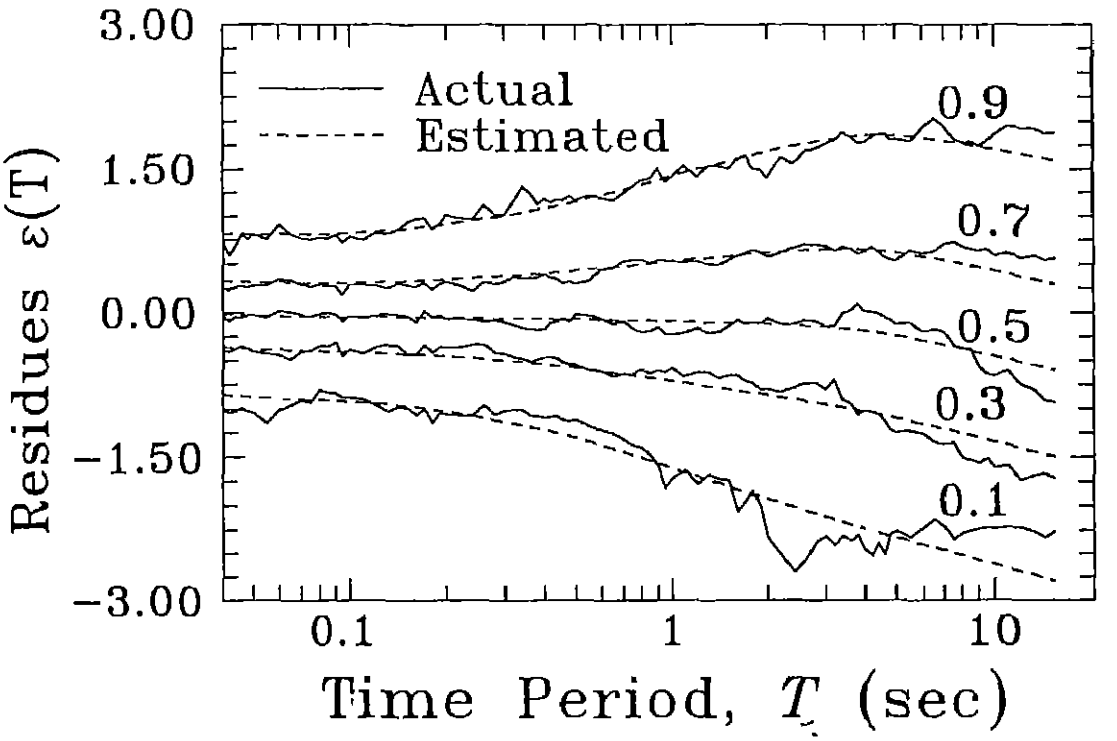

Figure 2.2(c) Residuals values for p, $p^* = 0.1$, 0.3, 0.5, 0.7 and 0.9 in Case of Hard Rock Site Condition.

residuals represent nice and smooth approximations for the actual residuals. The estimated residual values for nine different probability levels have been presented in Tables 2 2(a) to 2 2(c) respectively for the three site conditions

The KS statistics, $KS(T)$, and the chi-square statistics, $\chi^2(T)$, at each period, T, have been compared with their respective 95% cut-off levels (represented by the dashed lines) for all the three site conditions in Figs. 2 3(a) and 2 3(b) respectively. From Fig. 2.3(a), it is seen that except for the long periods, the computed KS statistics are well within the cut-off level for the alluvium site condition case. The KS test has however passed at fewer points for the other two site conditions. Further, Fig. 2 3(b) shows that for intermediate site conditions, the results of chi-square test are in very good agreement with the hypothesis. For the hard rock case also, a good agreement exists except in case of a few high periods. The chi-square test has however failed to accept the hypothesis to be true in case of alluvium site conditions. It is seen from these results that the normal distribution may not be an ideal description of the error distribution at all time periods. However, since the hypothesis has passed through both the tests at several time periods, and since there appears to be a very good agreement between the actual and estimated residuals (see Figs. 2.2(a) to 2 2(c)), the error estimates based on the assumed normal distribution have been considered to be acceptable.

In order to compare the probabilistic estimates of PSDF with the actual PSDFs corresponding to the recorded data, three example cases have been considered. These correspond to (a) east component recorded at Gilroy # 3 station during the 1984 Morgan Hill Earthquake with $M = 6\,2$, $R = 38.9$ km, $H = 9.0$

Table 2.2(a) - Residual Values for Alluvium Site Condition

Period,	Probability Level, p								
T (sec)	0.1	0 2	0 3	0 4	0.5	0.6	0 7	0.8	0 9
0.04	-0.754	-0 458	-0 243	-0.061	0 108	0.279	0 461	0.676	0 973
0 065	-0.729	-0 443	-0.236	-0 060	0 104	0 268	0.444	0 651	0.938
0 11	-0.712	-0.430	-0.226	-0 053	0 109	0.271	0 444	0 648	0 930
0.19	-0 702	-0.420	-0 217	-0 044	0 117	0 278	0 451	0 654	0 936
0.34	-0.731	-0 438	-0.227	0 048	0 120	0 287	0 467	0 679	0 971
0.50	-0.786	-0 475	-0 249	-0 058	0 121	0 300	0 491	0 717	1 027
0.90	-0.920	-0.556	-0.295	-0 072	0 137	0 344	0.567	0 828	1 192
1.60	-1.089	-0 658	-0.345	-0 081	0.168	0 415	0 680	0 992	1.423
2.80	-1.357	-0.882	-0 436	-0 107	0 198	0 506	0.834	1 220	1 755
4 40	-1 661	-1.026	-0.566	-0.176	0 188	0 554	0.944	1 404	2 039
7.50	-1.955	-1.257	-0 753	-0.325	0 075	0.475	0.903	1 408	2 105
14.00	-2.046	-1.378	-0 895	-0 484	-0 102	0 282	0.693	1.176	1 844

Table 2.2(b) - *Residual Values for Intermediate Site Condition*

Period,	Probability Level, p								
T (sec)	0 1	0 2	0.3	0.4	0.5	0 6	0 7	0 8	0 9
0.04	-0.522	-0.347	-0 222	-0 115	-0.015	0 085	0.192	0.318	0 492
0.06	-0 543	-0.359	-0.226	-0.113	-0 007	0 009	0 212	0 345	0 529
0.11	-0.567	-0.375	-0 236	-0 117	-0.007	0 104	0 222	0 361	0 553
0.19	-0 577	-0.382	-0.242	-0.123	-0.011	0.100	0 220	0 363	0.555
0.34	-0.588	-0.390	-0 246	-0.125	-0 011	0 103	0.225	0 368	0 566
0.50	-0.625	-0.414	-0.263	-0.134	-0.013	0.108	0 237	0 389	0 599
0.90	-0.743	-0 495	-0.315	-0 162	-0.020	0.123	0.275	0 455	0 703
1.60	-0.917	-0 610	-0 387	-0.198	-0 021	0 156	0 345	0 567	0 876
2.80	-1.176	-0 779	-0.492	-0 248	-0 020	0.208	0.452	0 739	1 137
4 40	-1.443	-0.961	-0.612	-0 317	-0.040	0 237	0 533	0 881	1.363
7.50	-1 741	-1.187	-0.787	-0.447	-0.128	0.189	0.529	0 929	1.482
14.00	-1.957	-1.389	-0.978	-0 628	-0.302	0 024	0 373	0.785	1.354

Table 2.2(c) - Residual Values for Hard Rock Site Condition

Period,	Probability Level, p								
0.04	-0.850	-0 563	-0 356	-0 179	-0 015	0 149	0 326	0 533	0 820
0 065	-0 893	-0.601	-0 389	-0.210	-0 042	0 126	0.305	0 517	0.809
0.11	-0.933	-0 630	-0 411	-0 225	-0 051	0 123	0 309	0 528	0 831
0.19	-1.017	-0 686	-0 447	-0.244	-0.056	0 134	0 338	0.576	0 906
0.34	-1.164	-0 786	-0.513	-0 280	-0 064	0 154	0.387	0 660	1.039
0 50	-1 299	-0.877	-0 572	-0.313	-0 071	0.171	0 430	0.735	1 157
0.90	-1 561	-1.056	-0.690	-0 379	-0 090	0 201	0 512	0 877	1 383
1.60	-1.830	-1.239	-0 811	-0 448	-0 109	0 230	0 593	1 020	1 612
2.80	-2 081	-1 416	-0 936	-0 527	-0.147	0 235	0 644	1 124	1 789
4.40	-2.279	-1 567	-1.053	-0 616	-0.207	0.200	0 637	1 151	1 863
7.50	-2.492	-1.758	-1.228	-0 777	-0 354	0.065	0 516	1.046	1 780
14.00	-2.759	-2.008	-1 464	-1 003	-0.572	-0 141	0 320	0 864	1 614

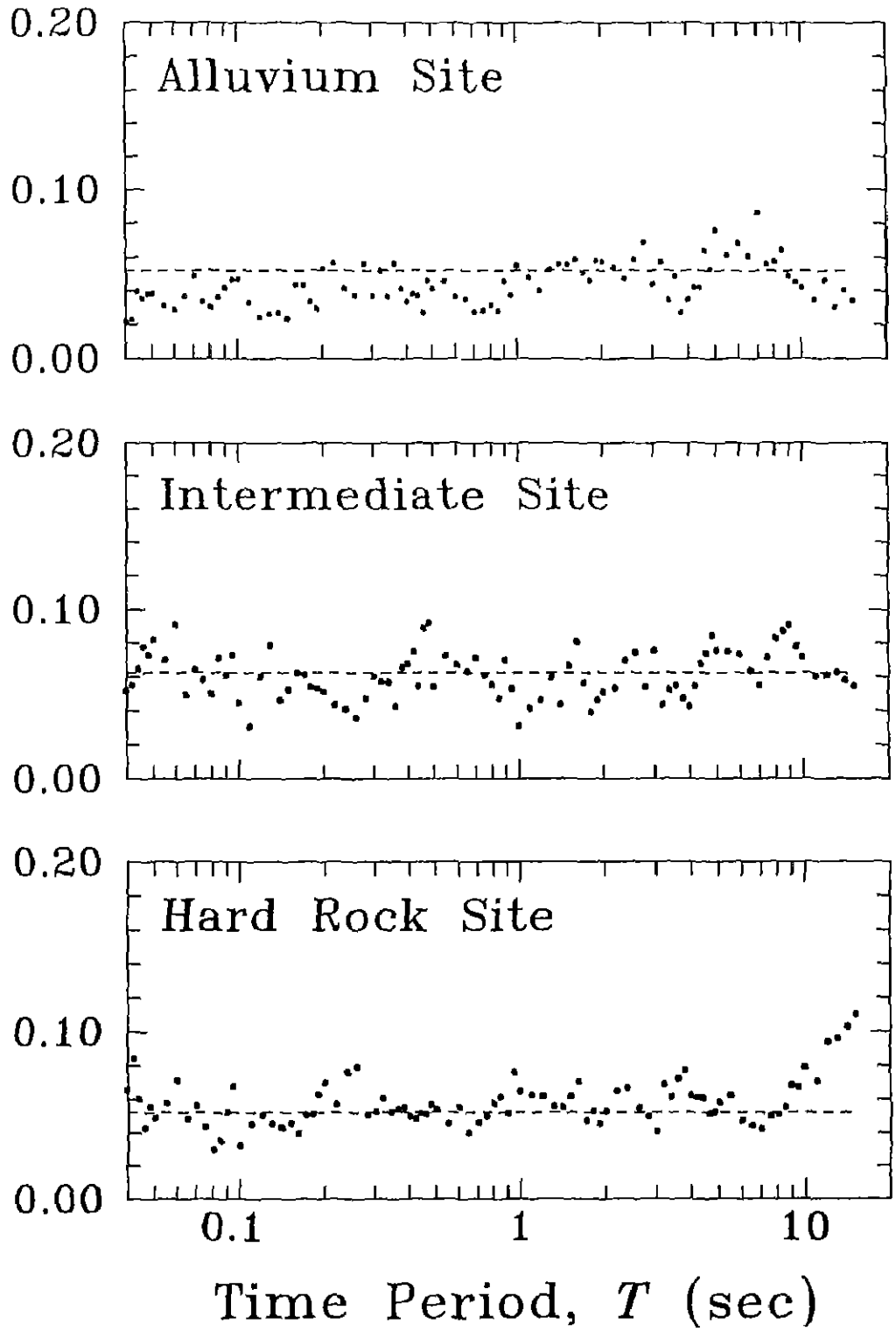

Figure 2.3(a) Comparison of KS Statistics at Different Time Periods with the 95% Cut-off Level for Different Site Categories.

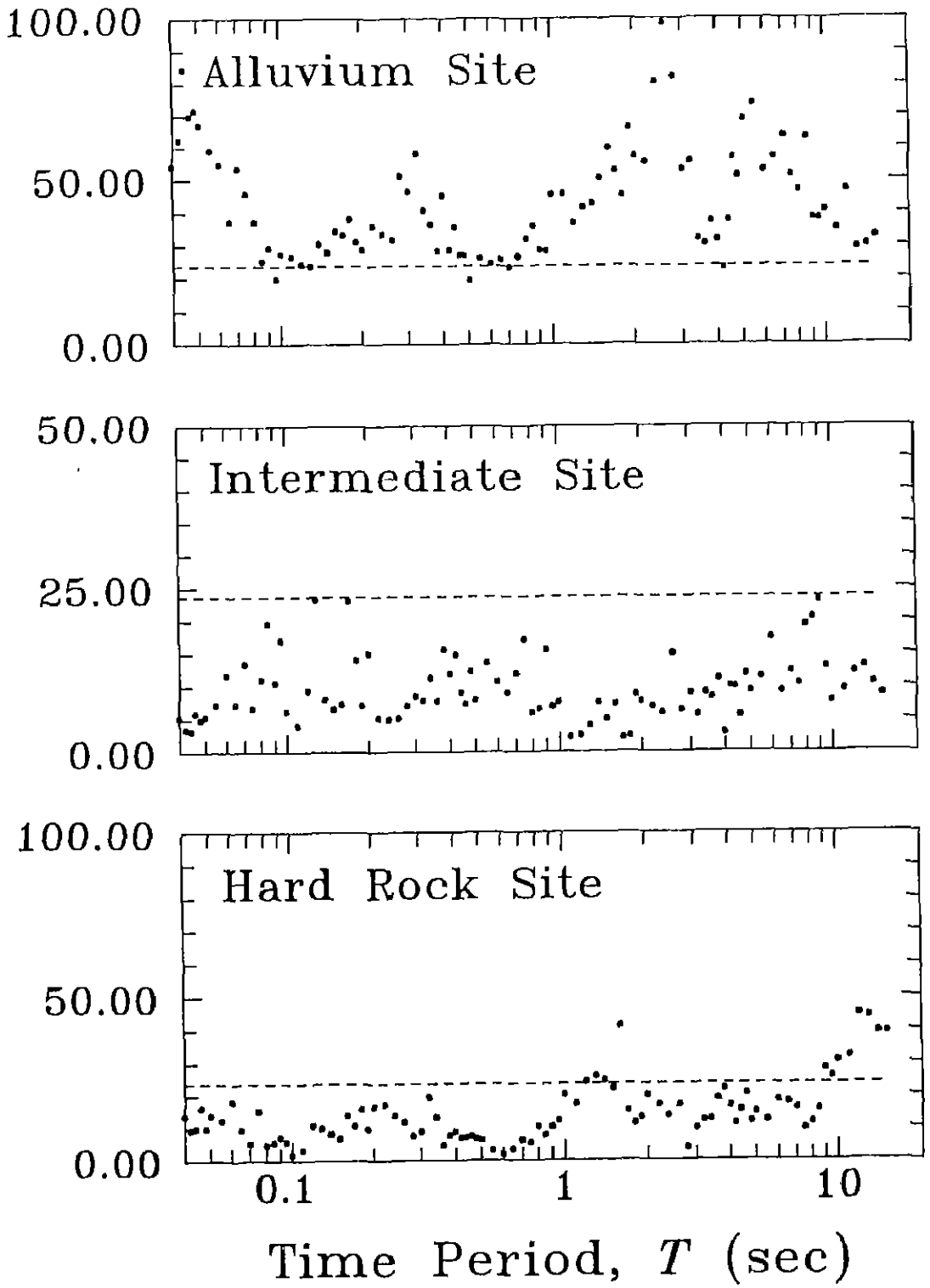

Figure 2.3(b) Comparison of Chi-square Statistics at Different Time Periods with the 95% Cut-off Level for Different Site Categories.

km, $s = 0$ and $T_s = 21\ 98$ sec, (b) south component recorded at Southern California Edison Company, Colton station during the 1970 Lytle Creek Earthquake with $M = 5\ 4$, $R = 31\ 5$ km, $H = 8\ 0$ km, $s = 1$ and $T_s = 10.60$ sec, and (c) S65E component recorded at Wrightwood station during the 1971 San Fernando Earthquake with $M = 6.4$, $R = 70\ 6$ km, $H = 13\ 0$ km, $s = 2$ and $T_s = 15\ 98$ sec. Figs. 2 4(a) to 2.4(c) respectively show the comparisons for these cases, with solid lines representing the estimated PSDFs corresponding to the probability levels, p = 0.1, 0.5 and 0.9 in each figure, and dashed lines representing the actual PSDFs. The estimated PSDFs have been obtained by using the least square estimates and error estimates as given in Tables 2 1(a) to 2 1(c) and Tables 2.2(a) to 2.2(c) respectively at 12 time periods. The region bounded by two extreme solid lines in each of the three figures represents the respective 80% confidence interval. It is seen that the actual PSDFs lie well within these confidence intervals Also, in the second and third example cases, the actual PSDFs are in good agreement with the estimated PSDFs for $p = 0.5$. However, the large uncertainty in the estimation of PSDFs as implied by the observed wide confidence intervals indicates that the proposed model needs to be improved further possibly with the inclusion of more earthquake source, path and site condition parameters.

To illustrate how PSDF changes with the variations in strong motion duration, earthquake magnitude, epicentral distance, and geologic site condition, Figs. 2.5 to 2.8 have been obtained by using the least square estimates and error estimates as given in Tables 2.1(a) to 2.1(c) and Tables 2.2(a) to 2.2(c) respectively at 12 time periods, and by taking focal depth, $H = 5$ km and p = 0.5. Fig. 2.5 shows the PSDFs for $T_s = 10$, 15, 20 and 25 sec in case of alluvium site conditions, with M and R respectively kept constant at 6 5 and

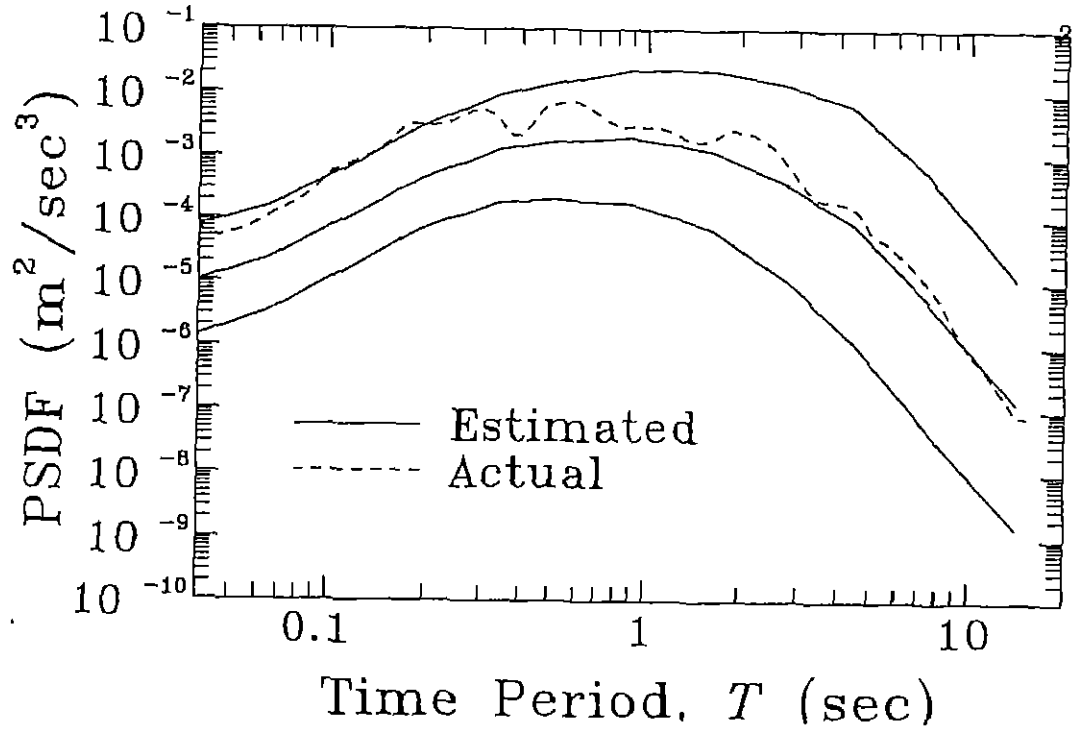

Figure 2.4(a) Comparison of Actual and Estimated PSDFs for Morgan Hill Earthquake Case.

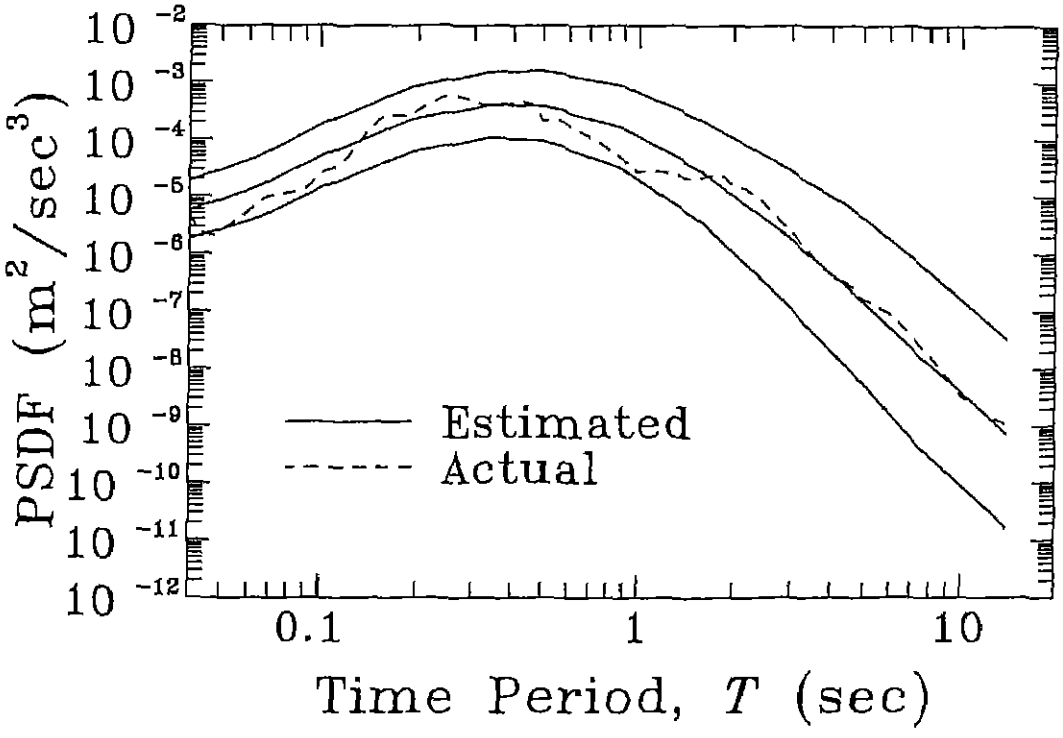

Figure 2.4(b) Comparison of Actual and Estimated PSDFs for Lytle Creek Earthquake Case.

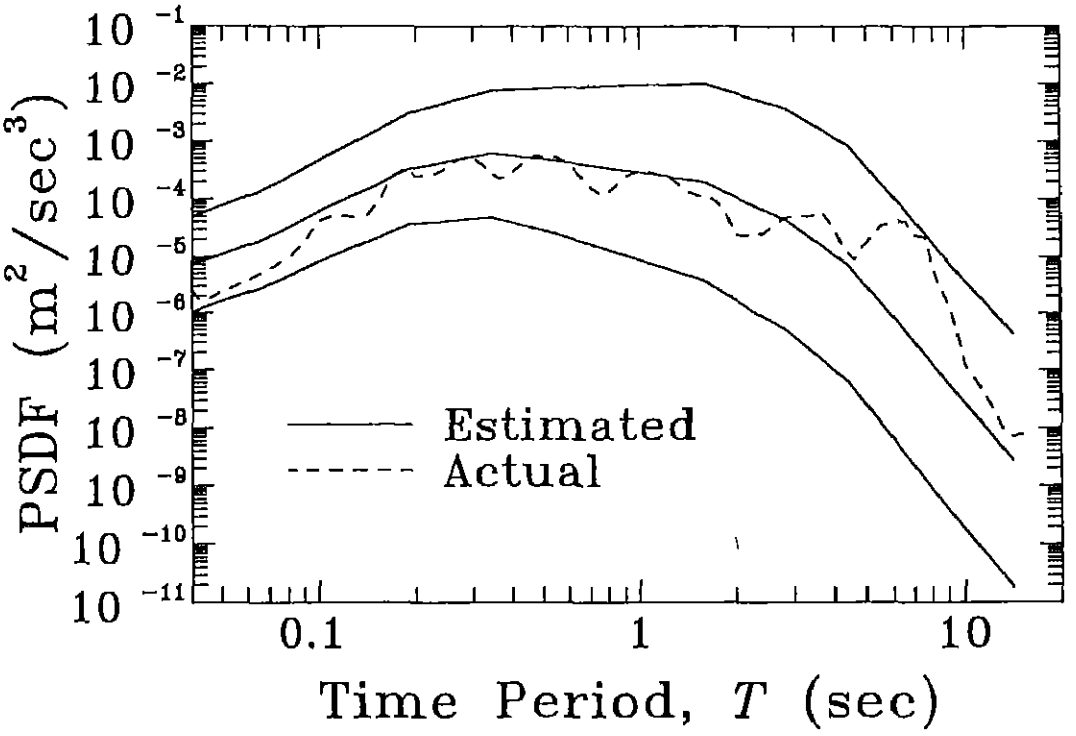

Figure 2.4(c) Comparison of Actual and Estimated PSDFs for San Fernando Earthquake Case.

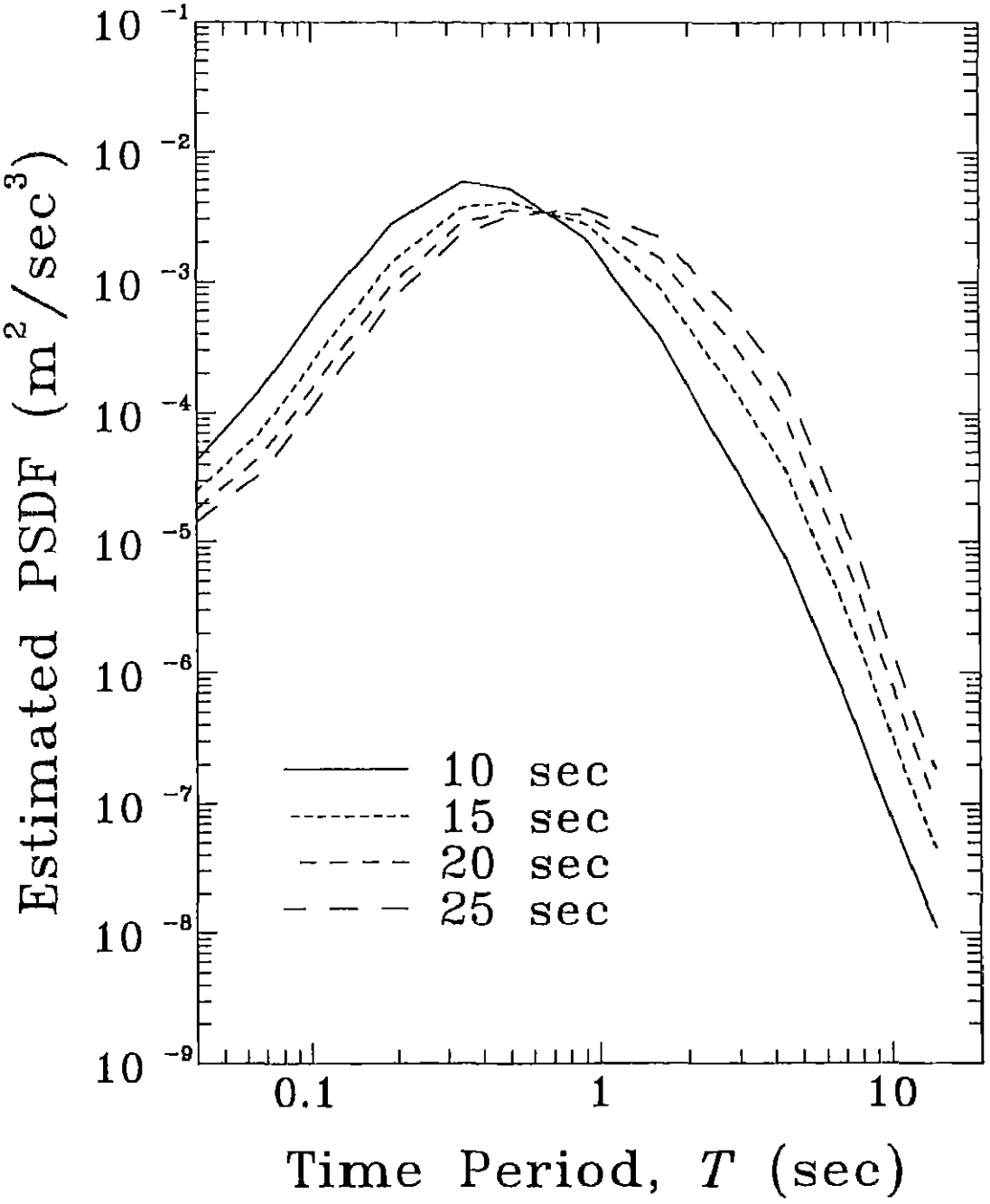

Figure 2.5 Estimated PSDFs for Different Durations in Case of Alluvium Site with $R = 50.0$ km, $H = 5.0$ km, $T_s = 20.0$ sec and $p = 0.5$.

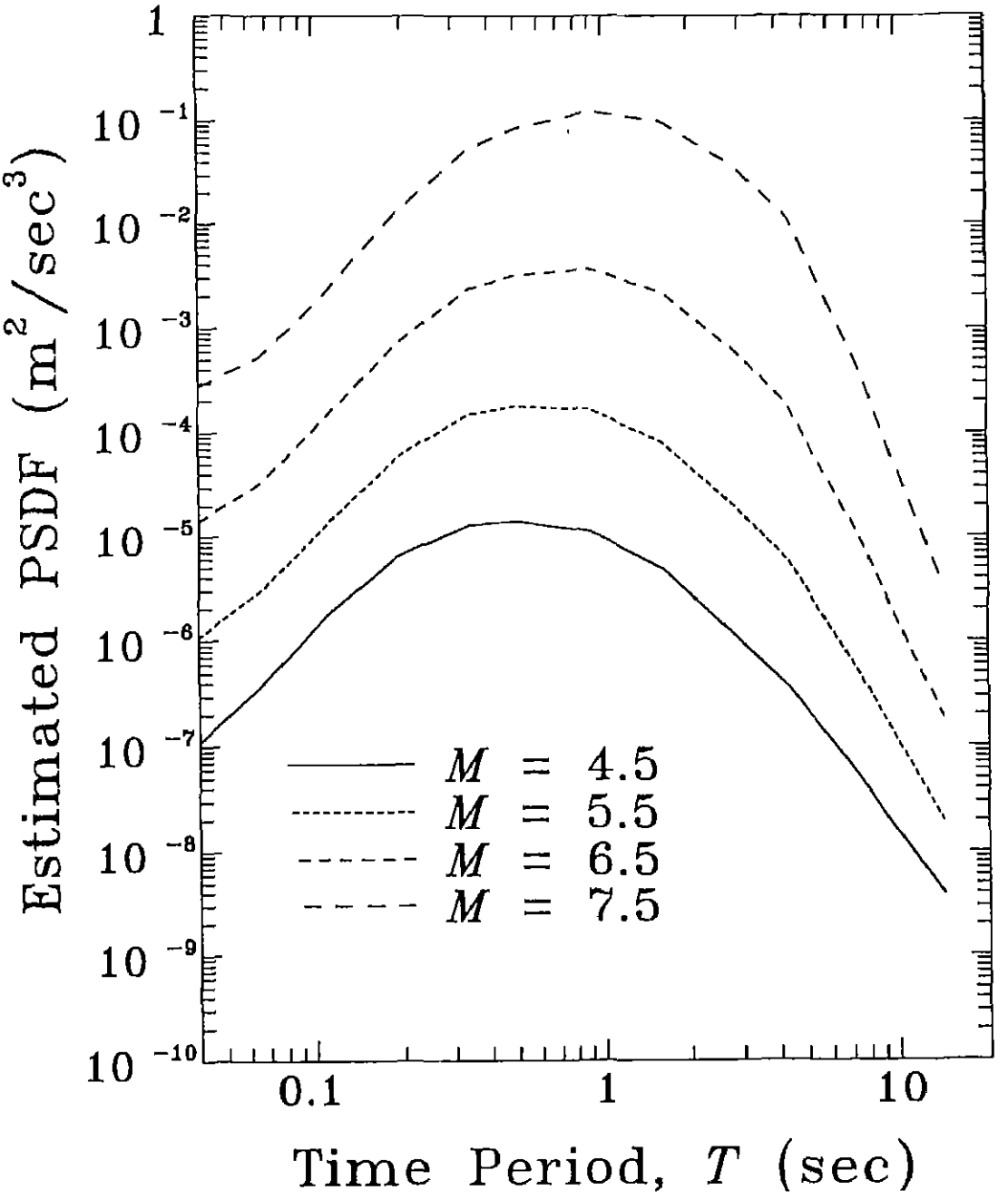

Figure 2.6 Estimated PSDFs for Different Magnitudes in Case of Alluvium Site with R = 50.0 km, H = 5.0 km, T_s = 20.0 sec and p = 0.5.

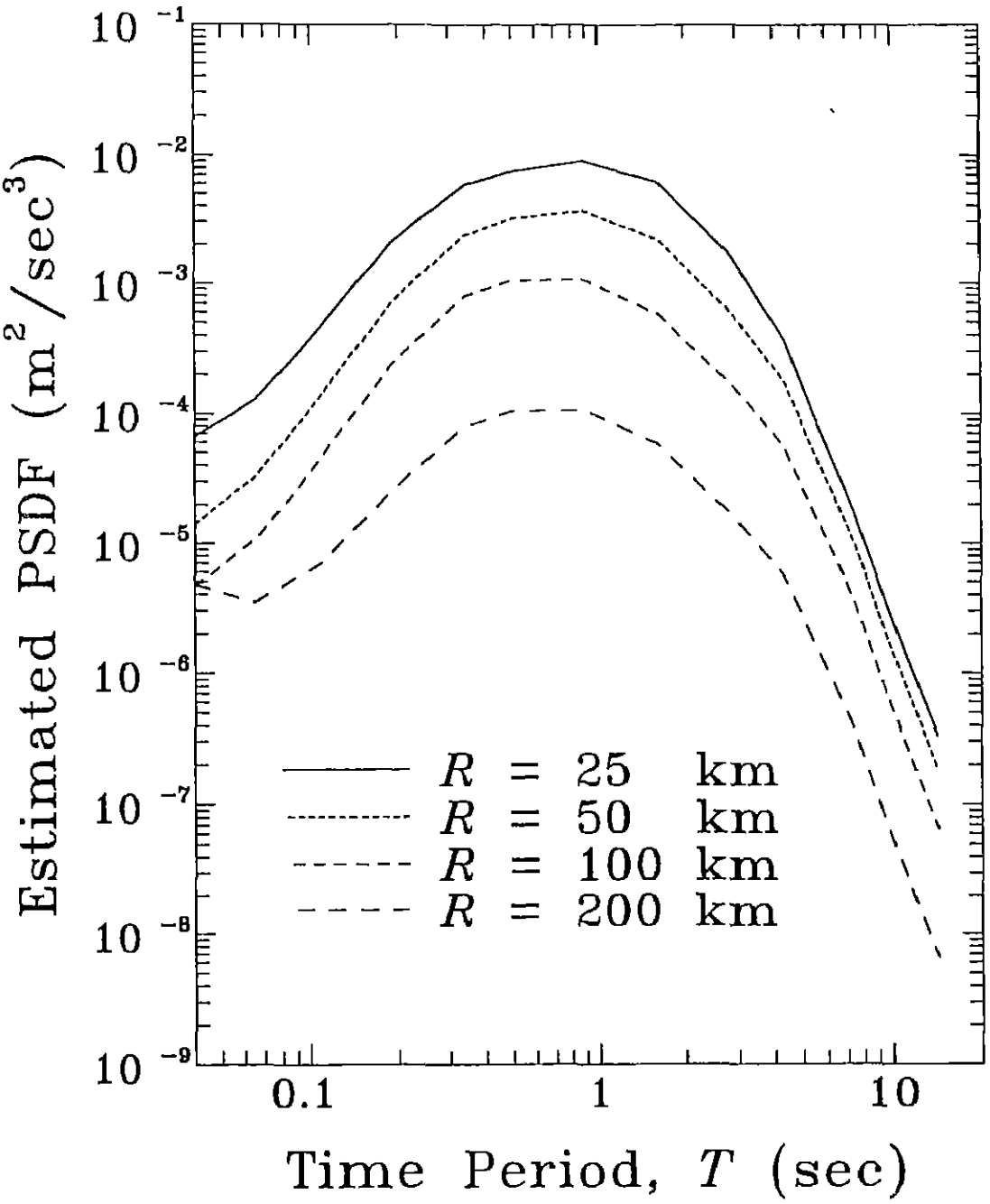

Figure 2.7 Estimated PSDFs for Different Epicentral Distances in Case of Alluvium Site with $M = 6.5$, $H = 5.0$ km, $T_s = 20.0$ sec and $p = 0.5$.

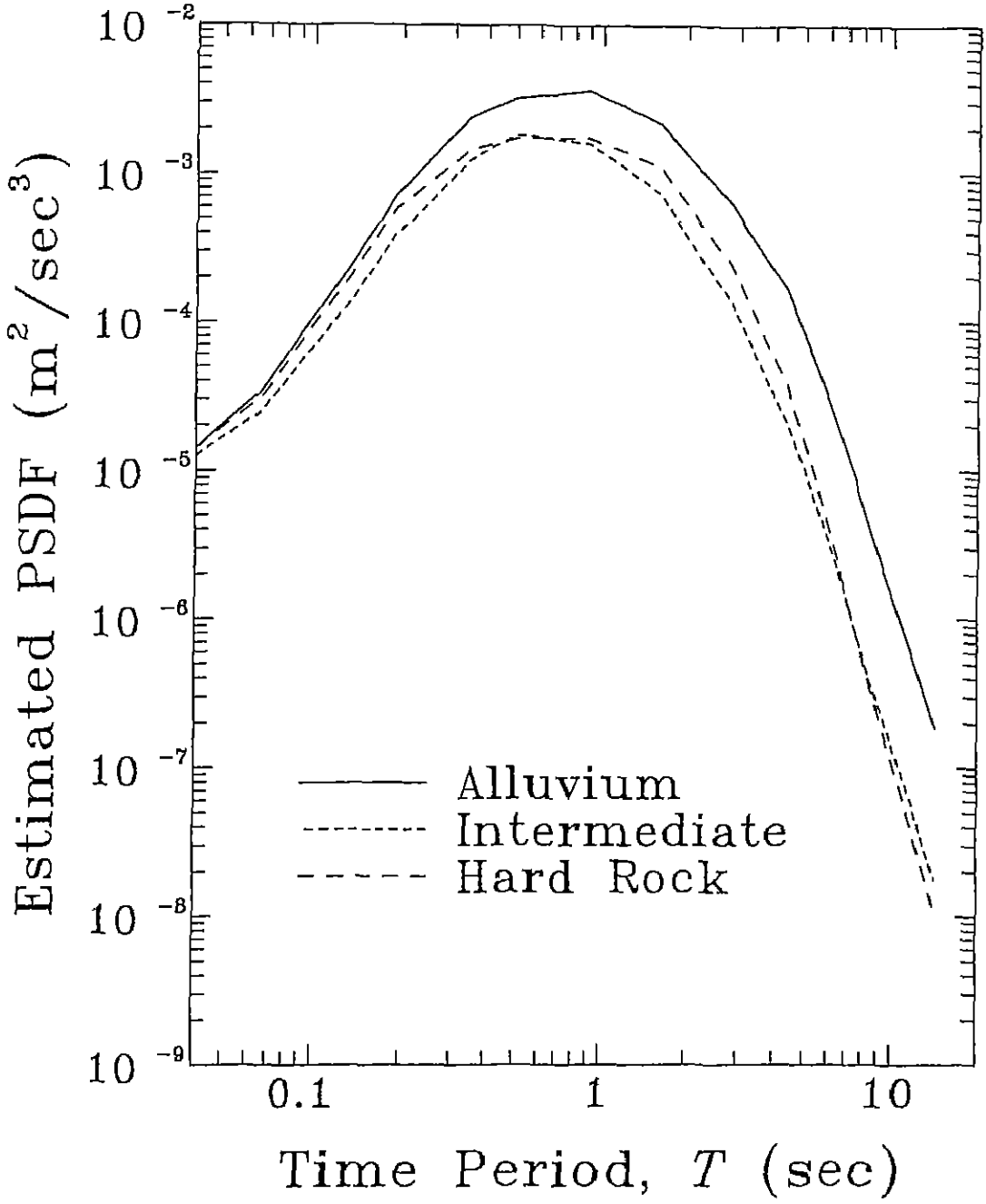

Figure 2.8 Estimated PSDFs for Different Site Conditions with $M = 6.5$, $R = 50.0$ km, $H = 5.0$ km, $T_s = 20.0$ sec and $p = 0.5$.

50 km Fig 2 6 shows the PSDFs for M = 4 5, 5.5, 6.5 and 7 5 in case of alluvium site conditions, with R and T_s respectively kept constant at 50 km and 20 sec. Fig 2 7 shows the PSDFs for R = 25, 50, 100 and 200 km in case of alluvium site conditions, with M and T_s kept constant at 6 5 and 20 sec Similarly, Fig 2 8 shows the PSDFs for the three site conditions, with the other parameters taken as M = 6 5, R = 50 km, and T_s = 20 sec. In any of these figures, however, a mutual comparison of various curves does not give a strictly true picture due to the observed correlations of strong motion duration with the other earthquake and site parameters (see Trifunac and Brady (1975b), Westermo and Trifunac (1978), Novikova and Trifunac (1994)). For example, in case of Fig. 2 6, it is unlikely that the events with different magnitudes will lead to 20 sec of strong motion duration with no change in the other parameters. In fact, it has been observed that the large magnitude earthquakes may cause longer ground motions at a site and thus, a comparison of various curves in Fig. 2 6 will be complete only when a higher value of T_s is associated with a larger value of M. Observing from Fig. 2.5 that the PSDF for a longer strong motion duration ground motion is likely to be richer in longer period waves, the shifting of the peaks to the longer periods with increasing M as in Fig. 2.6 may be actually more pronounced. This is consistent with the observation of Trifunac and Lee (1985b) that large magnitude earthquakes are dominated by the longer period waves. Same trend should also be obtained with the increasing epicentral distances from a simultaneous look at Figs. 2.5 and 2.7, even though the curves in Fig. 2.7 indicate that the 0.9–1.0 sec period waves should dominate the ground motions at all the considered epicentral distances.

CHAPTER III

SCALING RELATIONSHIPS AND AVERAGE SHAPES FOR NORMALIZED PSDF

3.1 Brief Overview

In the previous chapter, a scaling model was presented for the PSDF of horizontal earthquake ground motions and scaling coefficients were determined for three different site conditions through regression analysis. This model employed earthquake magnitude, epicentral distance, focal depth and strong ground motion duration as the governing parameters. In this chapter, the scaling model has been presented for the PSDF normalized to fixed values of PGA and ground motion duration. As in the previous model, this model explicitly includes the effect of earthquake magnitude, epicentral distance and focal depth for three different geologic site conditions. In a further simplification of this model, the 'average' PSDF curves corresponding to three different site conditions have been obtained and simple analytical forms have been proposed for these curves.

3.2 Scaling Equation and Regression Analysis

It is a common engineering practice to describe the severity of ground shaking at a site by PGA in a preliminary manner. In fact, PGA is the sole basis of seismic zonation in various countries around the world, even though this concept is slowly becoming outdated (Trifunac (1992)). Due to this reason, the design spectrum curves are usually specified as conditional to a predetermined

value of PGA For conformity with the existing practice, it has been considered desirable to also obtain the scaling equation of PSDF as conditional on PGA. It may be recalled here that the rms value of a ground acceleration process may be estimated by the square root of the area under the PSDF curve for the acceleration process, and that by multiplying this with a suitable peak factor, expected PGA may be estimated. It is therefore possible to scale the ordinates of a given PSDF uniformly so as to correspond to an expected predetermined value of PGA. Further, as mentioned in the previous chapters, there are several definitions of strong ground motion duration available to the engineering community, and no consensus has been reached yet on a definition that can be used in all the applications Due to this reason, it has been a common practice among researchers to consider the ground motion duration arbitarily as 20 sec in various PSDF-based studies including those on the spectrum-compatible PSDFs It has also been observed from the data-set (as considered in Chapter II) that most of the times, the estimated strong ground motion durations as per the definition of Trifunac and Brady (1975b) is close to 20 sec On the other hand, the application of the scaling model presented in Chapter II may often be inconvenient due to difficulty in estimating the strong ground motion duration. Keeping these considerations in view, an alternative scaling model is proposed to be obtained from the PSDF data normalized to the same PGA of $1.0g$ and the same duration of 20 sec. It is obvious that for this model, ground motion duration ceases to be a governing parameter. Further, since the variation of PGA with epicentral distance correlates very well with the attenuation characteristics in a given region, the attenuation function as considered in Chapter II has been omitted from this

alternative model The proposed scaling equation can thus be expressed as

$$\log_{10} PSDF_{\mathrm{N}}(T) = 2M + b_1(T)M + b_2(T)D_h + b_3(T) + b_4(T)M^2 \qquad (3\ 1)$$

where, $PSDF_{\mathrm{N}}(T)$ denotes the PSDF normalized to $1.0g$ PGA and 20 sec duration, and $D_h = \sqrt{H^2 + R^2}$ is the hypocentral distance. It may be noted that the representative distance, Δ, as considered in the scaling relationship in Chapter II has been replaced by the hypocentral distance, D_h. This has been done for the simplicity in the model as the estimation of the fault-size, S, may not always be convenient in practical applications.

For the regression analysis, the raw PSDF data-set has been prepared from the response spectra corresponding to the recorded accelerograms as in Chapter II However, here the PSDF compatible with a response spectrum has been computed by taking the ground motion duration equal to 20 0 sec in all cases. Also, the 'average' PSDF (as obtained by averaging the PSDFs for three response spectra) for each recorded motion has been normalized to an expected PGA value of 1 $0g$. Let this be denoted by $PSDF_{\mathrm{N}}(T)$ The regression analysis has been performed for each site condition by following the same method as presented in the Chapter II. Data selection has also been performed prior to the regression analysis in a similar way except for carrying out the bubble sorting on the basis of $(\log_{10} PSDF_{\mathrm{N}}(T) - 2M)$ (in place of $(\log_{10} PSDF(T) - 2M - 2Att(\Delta, M, T))$) As mentioned in Chapter II, the data selection is aimed to minimize the 'bias' which might creep in the least square fitting due to uneven distribution of data among the magnitude classes and due to the relative abundance of data for some of the earthquake events.

Let the least square estimates of the coefficients, $b_1(T)$ through $b_4(T)$

in Eq (3 1), as obtained from the regression analysis at each period, T, and smoothed along the $\log_{10}T$ axis, be represented by $\hat{b}_1(T)$ through $\hat{b}_4(T)$ respectively. Thus, the least square estimate of $PSDF_{\rm N}(T)$ may be represented by $\widehat{PSDF}_{\rm N}(T)$ where

$$\log_{10}\widehat{PSDF}_{\rm N}(T) = 2M + \hat{b}_1(T)M + \hat{b}_2(T)D_{\rm h} + \hat{b}_3(T) + \hat{b}_4(T)M^2 \ . \qquad (3.2)$$

This equation is considered to be applicable only in the range, $M_{\rm min} \le M \le M_{\rm max}$, as described in Chapter II, where

$$M_{\rm min} = -\frac{\hat{b}_1(T)}{2\hat{b}_4(T)} \ , \qquad (3\ 3)$$

$$\text{and} \qquad M_{\rm max} = -\frac{2+\hat{b}_1(T)}{2\hat{b}_4(T)} \ . \qquad (3.4)$$

Thus, Eq. (3 2) may be modified to

$$\log_{10}\widehat{PSDF}_{\rm N}(T) = \begin{cases} 2M + \hat{b}_1(T)M_{\rm min} + \hat{b}_2(T)D_{\rm h} + \hat{b}_3(T) + \hat{b}_4(T)M_{\rm min}^2 \ ; & M \le M_{\rm min} \\ 2M + \hat{b}_1(T)M + \hat{b}_2(T)D_{\rm h} + \hat{b}_3(T) + \hat{b}_4(T)M^2 \ ; & M_{\rm min} \le M \le M_{\rm max} \\ 2M_{\rm max} + \hat{b}_1(T)M_{\rm max} + \hat{b}_2(T)D_{\rm h} + \hat{b}_3(T) + \hat{b}_4(T)M_{\rm max}^2 \ ; & M_{\rm max} \le M \ . \end{cases} \qquad (3.5)$$

Let the residual describing the deviation of the recorded normalized PSDF from the estimated value at period, T, be given by

$$\varepsilon(T) = \log_{10}PSDF_{\rm N}(T) - \log_{10}\widehat{PSDF}_{\rm N}(T) \ . \qquad (3.6)$$

Let the fluctuations in $\varepsilon(T)$ at period, T, for various PSDFs corresponding to a particular soil condition be assumed to be described by a Gaussion distribution with mean, $\mu(T)$, and standard deviation, $\sigma(T)$. Thus,

$$p(\varepsilon,T) = \frac{1}{\sigma(T)\sqrt{2\pi}} \int_{-\infty}^{\varepsilon(T)} \exp\Big[-\frac{1}{2}\Big(\frac{x-\mu(T)}{\sigma(T)}\Big)^2\Big]\mathrm{d}x \qquad (3.7)$$

is the probability of $\varepsilon(T)$ not being exceeded by the deviation at period, T. The actual probability, $p^*(\varepsilon, T)$, that $\varepsilon(T)$ will not be exceeded has been estimated at each of the 91 different periods, T, from the fractions of the residues as explained Chapter II. The assumed probability distribution function, $p(\varepsilon, T)$, has been then fitted to the actual distribution function at period, T with the determination of the least square estimates, $\hat{\mu}(T)$ and $\hat{\sigma}(T)$, of the mean and standard deviation respectively for each soil condition. Each set of the estimates, $\hat{\mu}(T)$ and $\hat{\sigma}(T)$, has been smoothed out along the $\log_{10}T$ axis for estimating (normalized) PSDF from the smoothed estimates, $\hat{b}_1(T)$, $\hat{b}_2(T)$, $\hat{b}_3(T)$ and $\hat{b}_4(T)$, with a given level of confidence. The chi-square statistics, $\chi^2(T)$, and the Kolmogorov-Smirnov statistics, $KS(T)$, have also been computed at each time period and compared with the respective limits for 95% level to test the 'quality of fit' of the normal distribution function described by Eq (3 7)

3.3 Results and Discussion

Figs. 3.1(a) to 3 1(c) show the plots (in solid lines) of the smoothed least square estimates, $\hat{b}_1(T)$ through $\hat{b}_4(T)$, of the regression coefficients for the alluvium site, the intermediate site and the hard rock site conditions respectively. In each graph, dashed lines delineate the 95% confidence interval for these coefficients. Tables 3.1(a) to 3.1(c) present the (smoothed) least square estimates, $\hat{b}_1(T)$ through $\hat{b}_4(T)$, and the (smoothed) values of the fitted normal distribution parameters, $\hat{\mu}(T)$ and $\hat{\sigma}(T)$, at 12 selected periods for the three site conditions. The corresponding residuals as estimated by using smoothed $\hat{\mu}(T)$ and $\hat{\sigma}(T)$ values respectively in place of $\mu(T)$ and $\sigma(T)$ in Eq. (3.7), have been tabulated in Tables 3.2(a) to 3.2(c) for nine different confidence levels. Figs. 3 2(a) to 3.2(c)

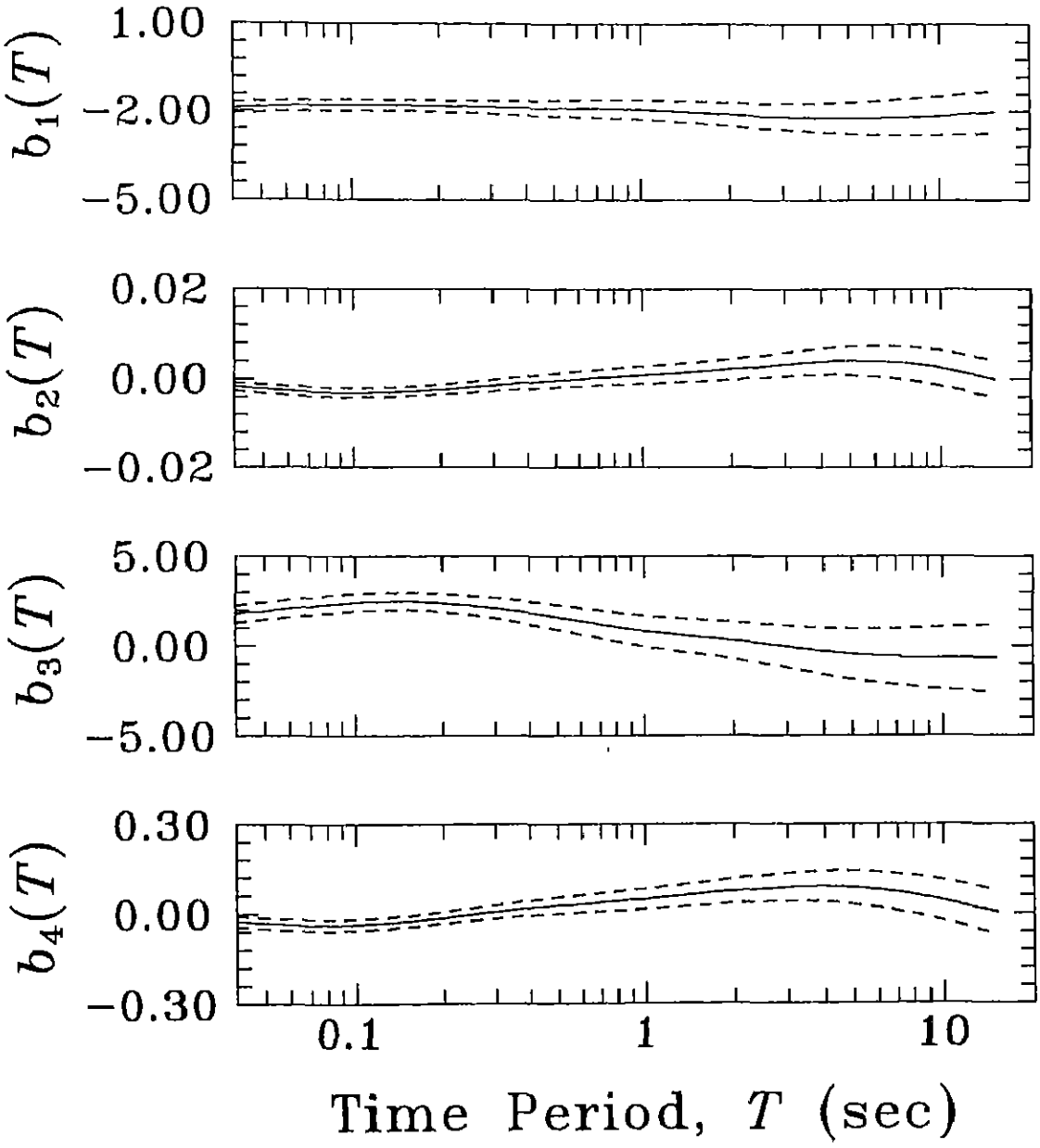

Figure 3.1(a) Regression Coefficients for Alluvium Site Condition.

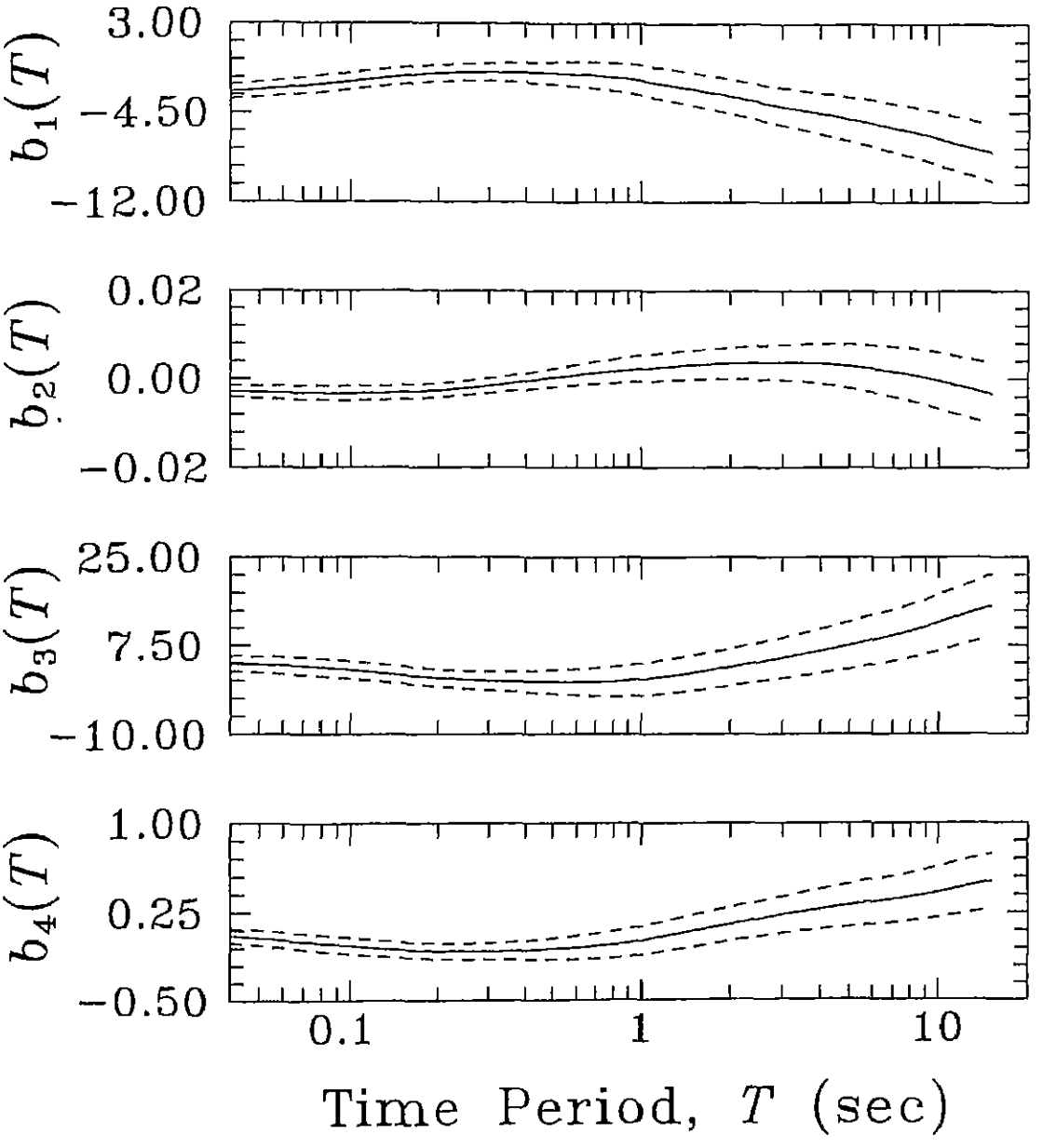

Figure 3.1(b) Regression Coefficients for Intermediate Site Condition.

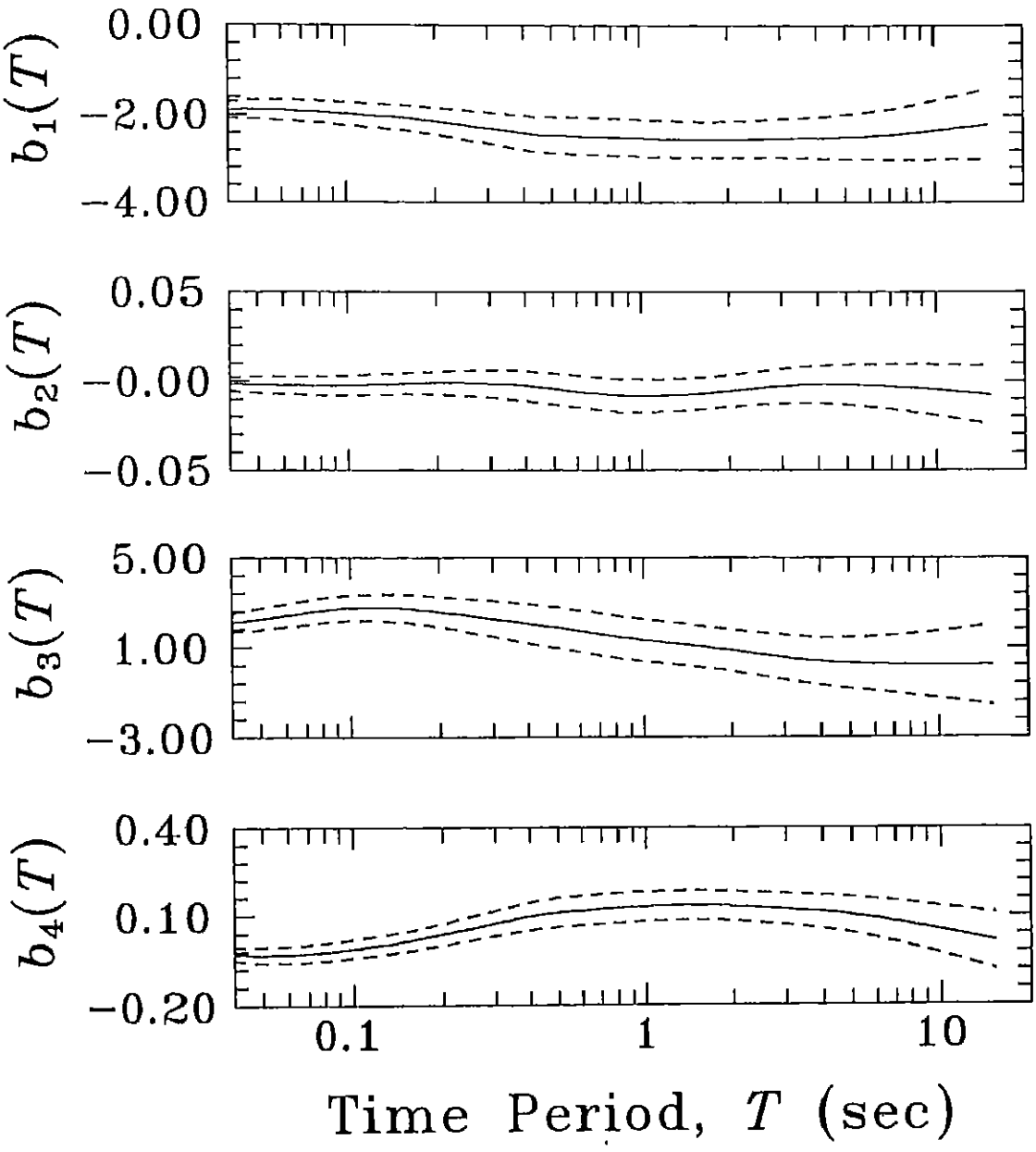

Figure 3.1(c) Regression Coefficients for Hard Rock Site Condition.

Table 3.1(a) - Least Square Estimates of Regression Coefficients and Residual Parameters for Alluvium Site Condition

Period,	Least Square Estimates of Regression Coefficients				Residual Parameters	
T (sec)	$\hat{b}_1(T)$	$100\hat{b}_2(T)$	$\hat{b}_3(T)$	$10\hat{b}_4(T)$	$\hat{\mu}(T)$	$\hat{\sigma}(T)$
0.04	-1.890	-0.172	1.800	-0.248	0.007	0.304
0.065	-1.830	-0.273	2.170	-0.364	-0.014	0.335
0.11	-1.800	-0.308	2.470	-0.339	-0.007	0.340
0.19	-1.830	-0.215	2.440	-0.150	0.016	0.324
0.34	-1.880	-0.118	2.030	0.127	0.031	0.358
0.50	-1.900	-0.033	1.630	0.276	0.038	0.415
0.90	-1.930	0.070	0.944	0.456	0.057	0.515
1.60	-2.050	0.168	0.448	0.675	0.074	0.627
2.80	-2.170	0.304	0.041	0.853	0.089	0.825
4.40	-2.230	0.403	-0.361	0.892	0.081	1.051
7.50	-2.200	0.355	-0.614	0.659	0.038	1.271
14.00	-2.040	0.036	-0.672	0.095	0.006	1.421

Table 3.1(b) - Least Square Estimates of Regression Coefficients and Residual Parameters for Intermediate Site Condition

Period,	Regression Coefficients				Residual Statistics	
T (sec)	$\hat{b}_1(T)$	$100\hat{b}_2(T)$	$\hat{b}_3(T)$	$10\hat{b}_4(T)$	$\hat{\mu}(T)$	$\hat{\sigma}(T)$
0 04	-2.730	-0 277	3.850	0 604	0 001	0 267
0 065	-2 360	-0 321	3 440	0.179	0 002	0 297
0 11	-1 790	-0 331	2 400	-0 341	0 003	0 302
0 19	-1 250	-0 278	1 100	-0 717	0 006	0.290
0 34	-1.090	-0 123	0 384	-0 705	-0 001	0 318
0.50	-1 170	0.017	0 240	-0.541	-0 018	0.386
0 90	-1.580	0 200	0 488	-0 017	-0 049	0.514
1.60	-2.620	0 319	2.250	1 080	-0 069	0 613
2 80	-3.800	0.365	4 670	2 170	-0 073	0.708
4.40	-4.740	0 331	6.850	2 930	-0.077	0.813
7.50	-5.900	0.135	9 960	3.700	-0.079	0.976
14.00	-7.680	-0.279	14 900	4 960	-0.069	1.234

Table 3.1(c) - Least Square Estimates of Regression Coefficients and Residual Parameters for Hard Rock Site Condition

Period,	Least Square Estimates of Regression Coefficients				Residual Statistics	
T (sec)	$\hat{b}_1(T)$	$100\hat{b}_2(T)$	$\hat{b}_3(T)$	$10\hat{b}_4(T)$	$\hat{\mu}(T)$	$\hat{\sigma}(T)$
0 04	-1 900	-0.173	2 120	-0 274	-0.017	0 260
0.065	-1 910	-0 255	2 490	-0 276	0 010	0.338
0 11	-2 000	-0 239	2 760	-0 051	0.024	0 372
0.19	-2 140	-0 133	2 600	0 329	0 014	0.434
0 34	-2 350	0 207	2.180	0 852	-0 014	0 565
0 50	-2.460	-0.456	1 880	1.110	-0 034	0 629
0 90	-2.520	-0.836	1.400	1 290	-0.063	0.636
1.60	-2.570	-0.705	1 030	1.340	-0 063	0.593
2.80	-2 540	-0 339	0 601	1 230	-0 036	0.612
4 40	-2.520	-0 196	0 343	1.080	-0 009	0 683
7.50	-2.430	-0.366	0 241	0.740	0.027	0 818
14 00	-2.240	-0 745	0 221	0 203	0.076	1 046

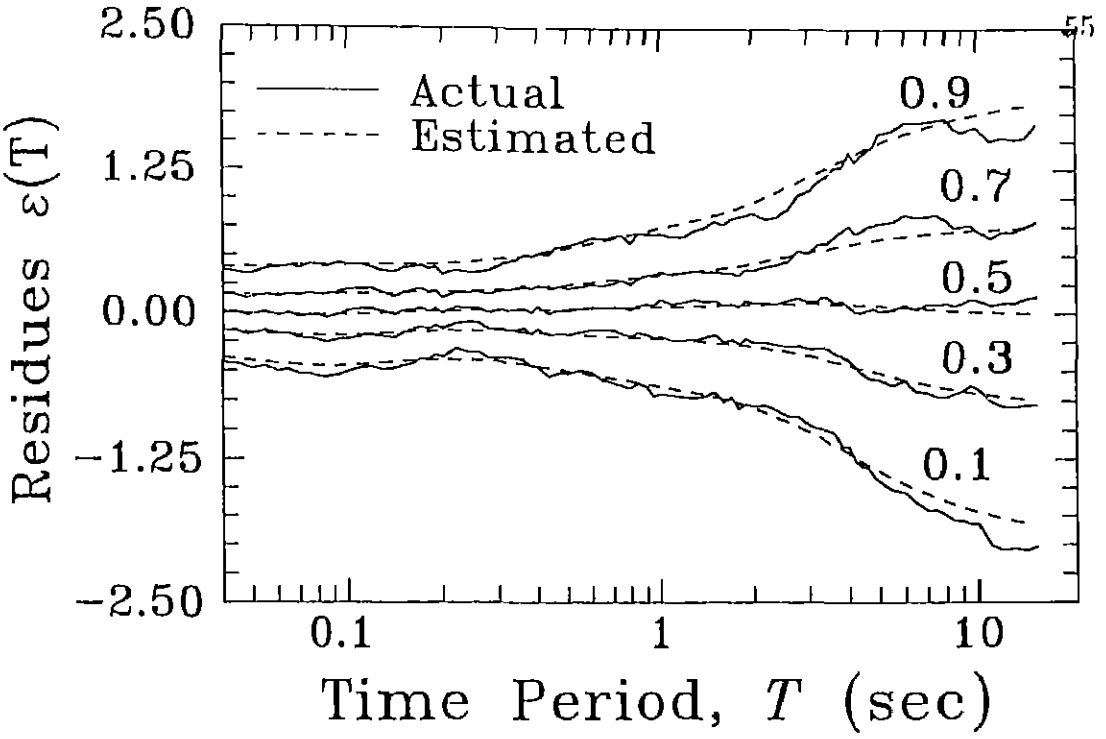

Figure 3.2(a) Residuals for p, $p^* = 0.1, 0.3, 0.5, 0.7$ and 0.9 in Case of Alluvium Site Condition.

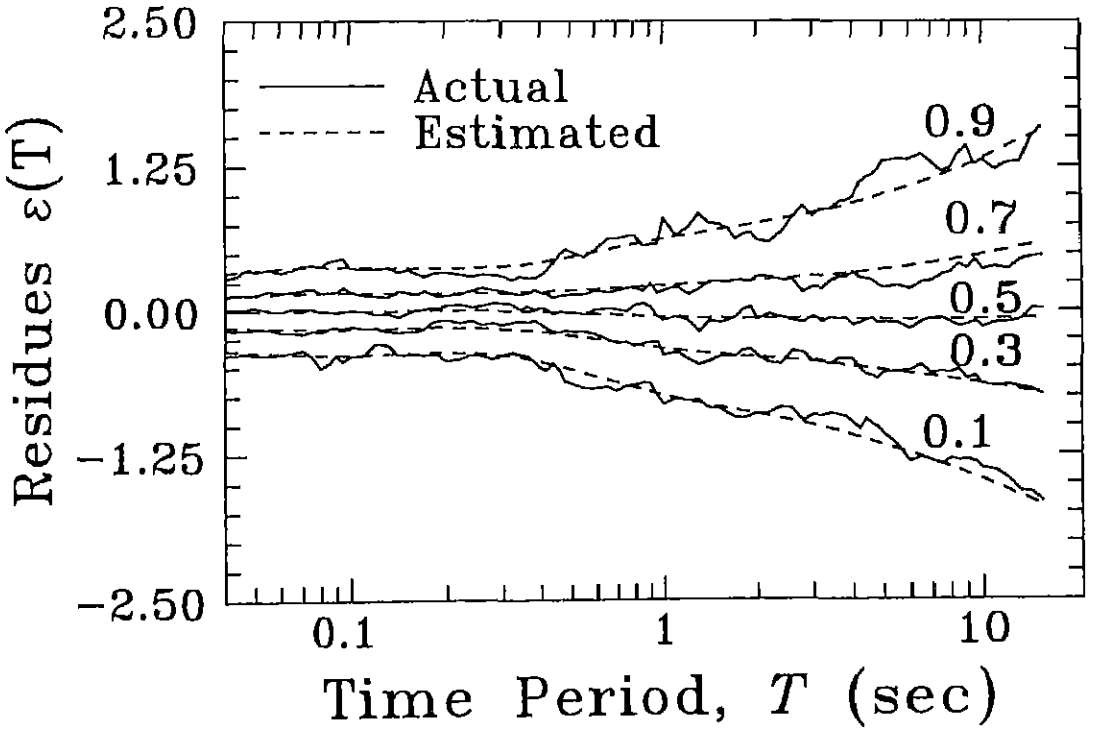

Figure 3.2(b) Residuals for p, $p^* = 0.1, 0.3, 0.5, 0.7$ and 0.9 in Case of Intermediate Site Condition.

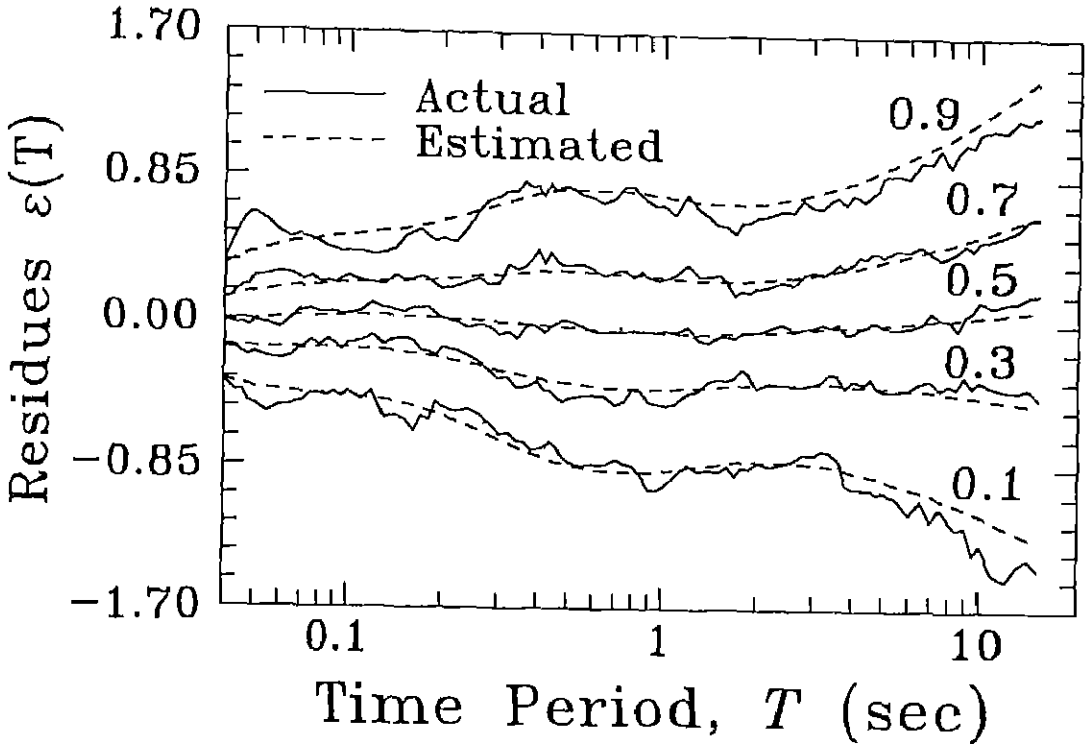

Figure 3.2(c) Residuals values for p, $p^* = 0.1$, 0.3, 0.5, 0.7 and 0.9 in Case of Hard Rock Site Condition.

Table 3.2(a) - Residual Values for Alluvium Site Condition

Period,	Probability Level, p								
T (sec)	0.1	0.2	0.3	0.4	0 5	0.6	0 7	0 8	0 9
0 04	-0.383	-0 249	-0 152	-0.070	0 007	0.084	0 166	0 263	0.397
0 065	-0.444	-0.296	-0.189	-0 099	-0 014	0 071	0 161	0 268	0 416
0.11	-0.443	-0.293	-0.185	-0.090	-0.007	0.079	0 171	0.279	0.429
0 19	-0.400	-0.257	-0 154	-0 066	0 016	0 098	0.185	0 289	0 431
0.34	-0 428	-0.270	-0 156	-0 060	0 031	0 121	0.218	0 332	0 490
0.50	-0.494	-0 312	-0 179	-0 067	0.038	0 143	0 255	0 387	0 571
0.90	-0.604	-0.377	-0 213	-0 073	0 057	0.187	0.327	0 491	0 718
1.60	-0.730	-0.454	-0.254	-0.084	0 075	0.233	0 402	0 602	0 878
2.80	-0.969	-0 606	-0.343	-0.119	0 089	0 298	0 521	0 784	1 147
4 40	-1 267	-0.804	-0 469	-0 184	0.082	0.347	0.631	0.966	1 429
7.50	-1 592	-1 032	-0 627	-0 283	0.038	0 359	0 703	1 108	1.668
14.00	-1 816	-1 190	-0 737	-0.353	-0 005	0 365	0 750	1 202	1 828

Table 3.2(b) - Residual Values for Intermediate Site Condition

Period,	Probability Level, p								
T (sec)	0.1	0.2	0 3	0.4	0.5	0.6	0.7	0 8	0.9
0 04	-0 341	-0.224	-0.139	-0.067	0 001	0.068	0 141	0 226	0 343
0 065	-0.379	-0.248	-0 153	-0.073	0 002	0 077	0.157	0 252	0 383
0.11	-0 384	-0 251	-0 155	-0 073	-0 003	0 079	0.161	0 257	0 396
0 19	-0 366	-0 238	-0 146	-0 067	0.006	0.079	0 158	0 250	0 378
0 34	-0.409	-0.269	-0.167	-0.081	-0 001	0 079	0 165	0 267	0 407
0.50	-0 513	-0.343	-0 220	-0.116	-0 018	0 080	0 184	0 307	0 477
0.90	-0 708	-0 482	-0 318	-0 179	-0 049	0 081	0 220	0 384	0 611
1 60	-0.855	-0 585	-0 390	-0 224	-0 069	0 086	0 252	0 447	0 717
2.80	-0.981	-0.669	-0 444	-0 252	-0.073	0 106	0 297	0 523	0 835
4.40	-1.120	-0 761	-0.503	-0 282	-0.077	0.129	0.349	0.608	0 966
7.50	-1.331	-0 901	-0.590	-0 326	-0 078	0.168	0 432	0 743	1.173
14 00	-1 651	-1 108	-0.715	-0 381	-0 069	0 243	0 577	0 970	1.514

Table 3.2(c) - Residual Values for Hard Rock Site Condition

Period,	Probability Level, p								
T (sec)	0.1	0.2	0.3	0 4	0.5	0 6	0 7	0.8	0 9
0 04	-0.350	-0 236	-0 153	-0.083	-0 017	0 049	0.119	0 202	0 316
0.065	-0 423	-0.275	-0.167	-0.075	0 010	0 095	0 187	0.294	0 443
0.11	-0.453	-0 289	-0.171	-0 070	0.024	0.118	0.219	0 337	0.501
0.19	-0 543	-0.351	-0 213	-0 096	0 014	0 124	0.241	0.379	0 571
0.34	-0.738	-0.490	-0 310	-0.157	-0 014	0 129	0.282	0 461	0.711
0.50	-0.840	-0.563	-0.363	-0.193	-0 034	0 125	0 295	0.495	0 773
0.90	-0 878	-0.598	-0.396	-0.224	-0 063	0 098	0 270	0 472	0 752
1 60	-0 823	-0.562	-0 373	-0.213	-0 064	0.087	0.247	0 436	0 697
2.80	-0.821	-0.551	-0 356	-0.191	-0.036	0 119	0 284	0 479	0.749
4.40	-0 885	-0.584	-0.366	-0 182	-0.009	0 164	0.348	0.566	0.867
7 50	-1.022	-0 661	-0 401	-0.180	0 027	0.234	0 455	0.715	1.076
14.00	-1 265	-0.804	-0.471	-0 188	0 076	0.340	0 623	0.956	1 417

show the comparisons of these residuals with the actual residuals for the alluvium site, intermediate site, and hard rock conditions respectively In each figure, the solid lines represent the actual residuals for $p^* = 0\,1$, 0.3, 0 5, 0 7 and 0 9 while the dashed lines represent the estimated residuals for $p = 0.1$, 0.3, 0.5, 0.7 and 0.9. A close agreement is observed between the actual and the estimated residuals for all the cases. To test this agreement further, let us look at the values of the $KS(T)$ and $\chi^2(T)$ statistics as shown in Figs. 3 3(a) and (b) respectively. These statistics are computed at each of the 91 time periods and compared with the critical values of KS and χ^2 tests for 95% confidence level (see the dashed lines) for each site condition. It is observed that the KS test passes for the alluvium site case at most of the periods, while in the other cases, this test passes at fewer periods as for the previous scaling model It is also observed from Fig 3 3(b) that for these site conditions, in most of the periods, the chi-square test does not reject the hypothesis that the error distribution is normal. For the alluvium site condition, however, this test fails at most of the time periods As indicated by these test results, the normal distribution may not be an ideal distribution However, in view of the fact that the results for a particular site condition are passing one of these tests, normal distribution has been accepted to be the reasonable distribution for describing the residual estimates.

In order to illustrate how the probabilistic estimates of (normalized) PSDF compare with the actual PSDFs, same three example cases have been considered as in Chapter II. Figs. 3 4(a) to 3.4(c) show these comparisons respectively for the Morgan Hill Earthquake case, Lytle Creek Earthquake case, and San Fernando Earthquake case, with solid lines representing the estimated PSDFs corresponding to the probability levels, $p = 0.1$, 0 5 and 0.9 in each figure,

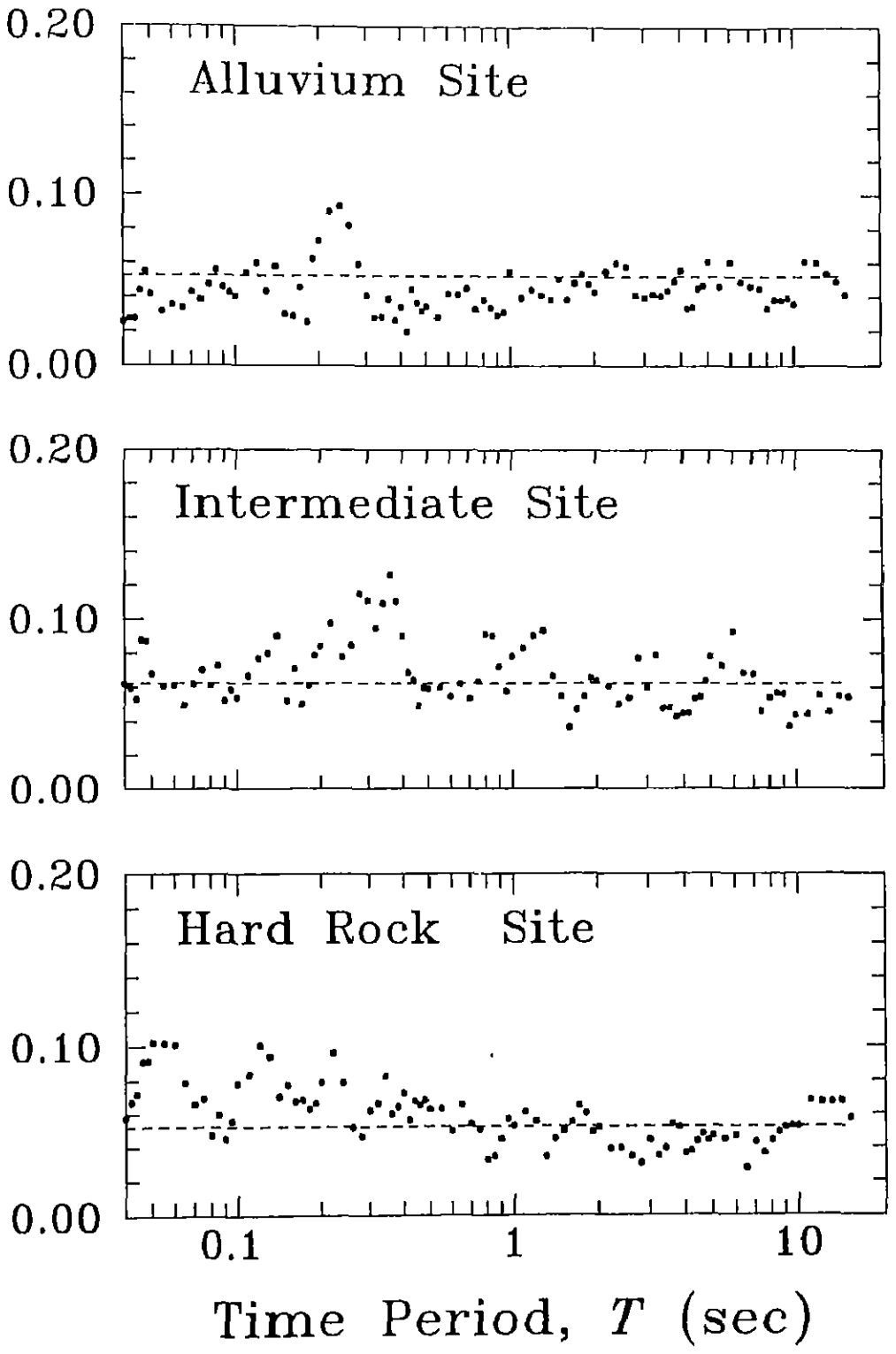

Figure **3.3(a)** Comparison of KS Statistics at Different Time Periods with the 95% Cut-off Level for Different Site Categories.

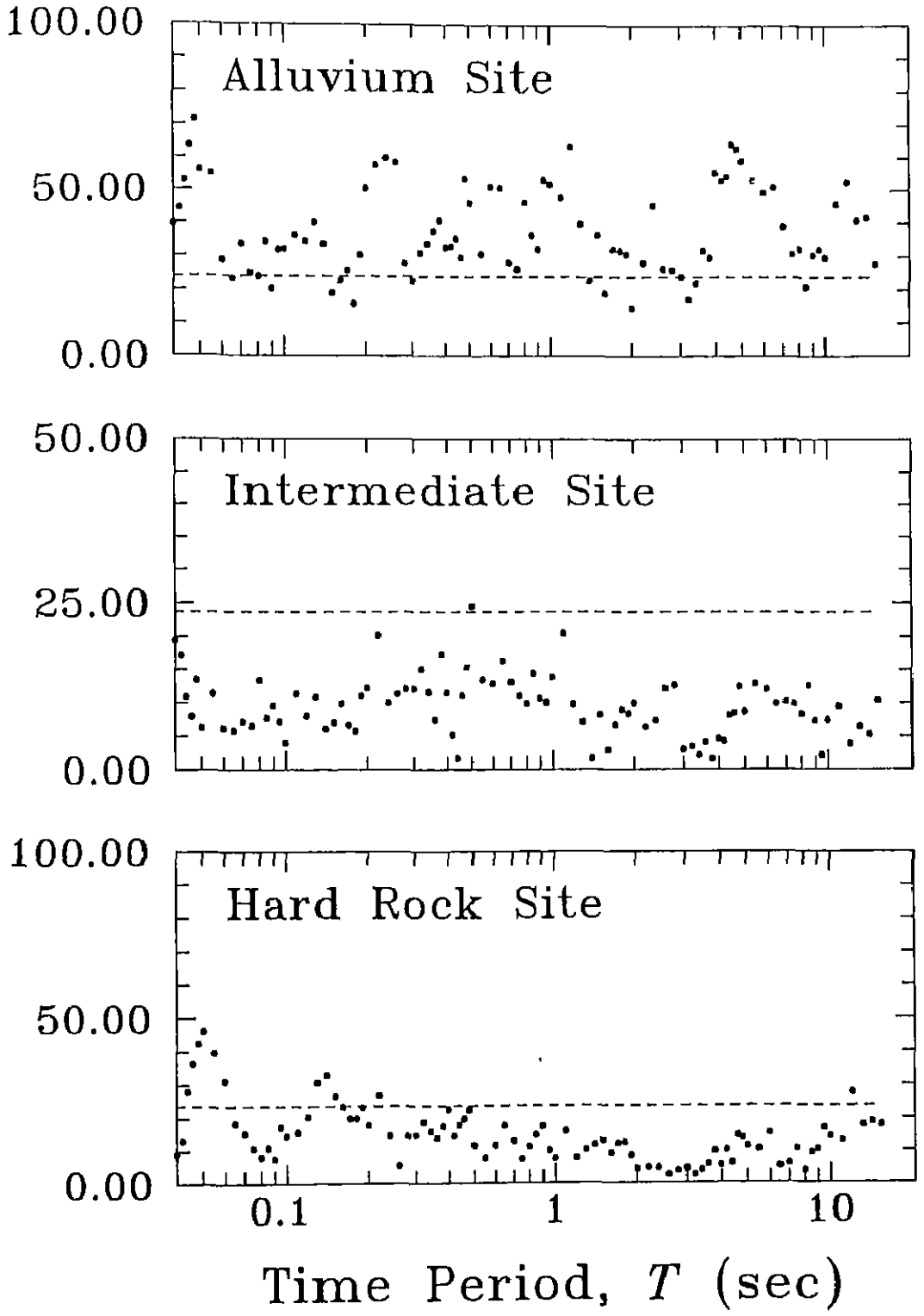

Figure 3.3(b) Comparison of Chi-square Statistics at Different Time Periods with the 95% Cut-off Level for Different Site Categories.

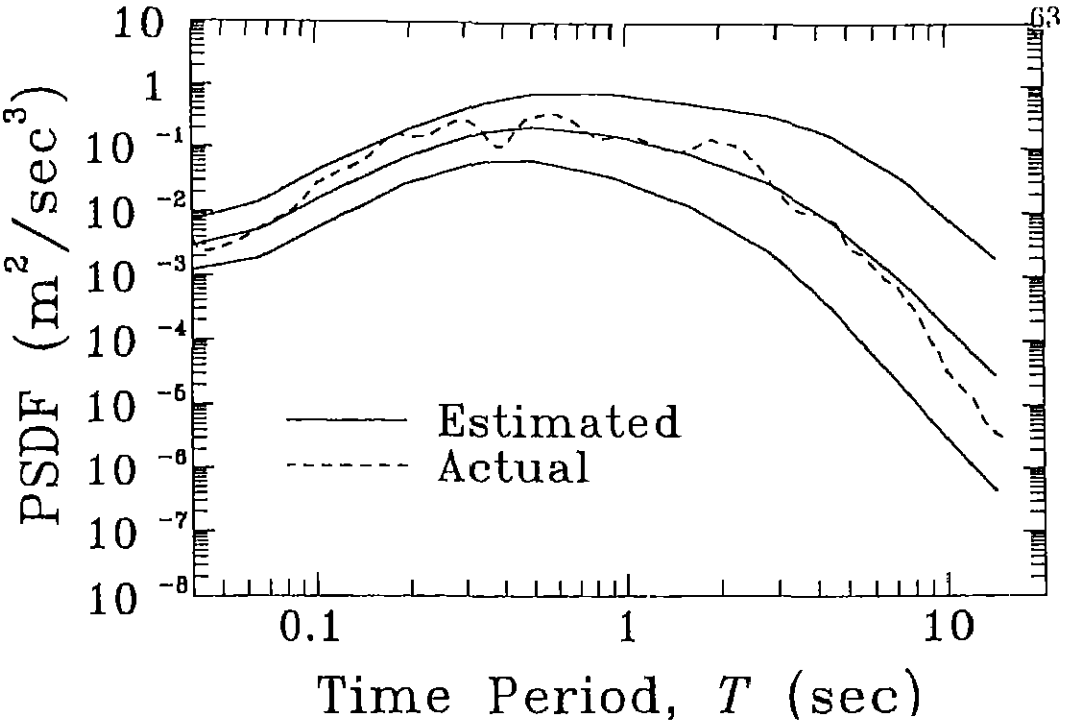

Figure 3.4(a) Comparison of Actual and Estimated PSDFs for Morgan Hill Earthquake Case.

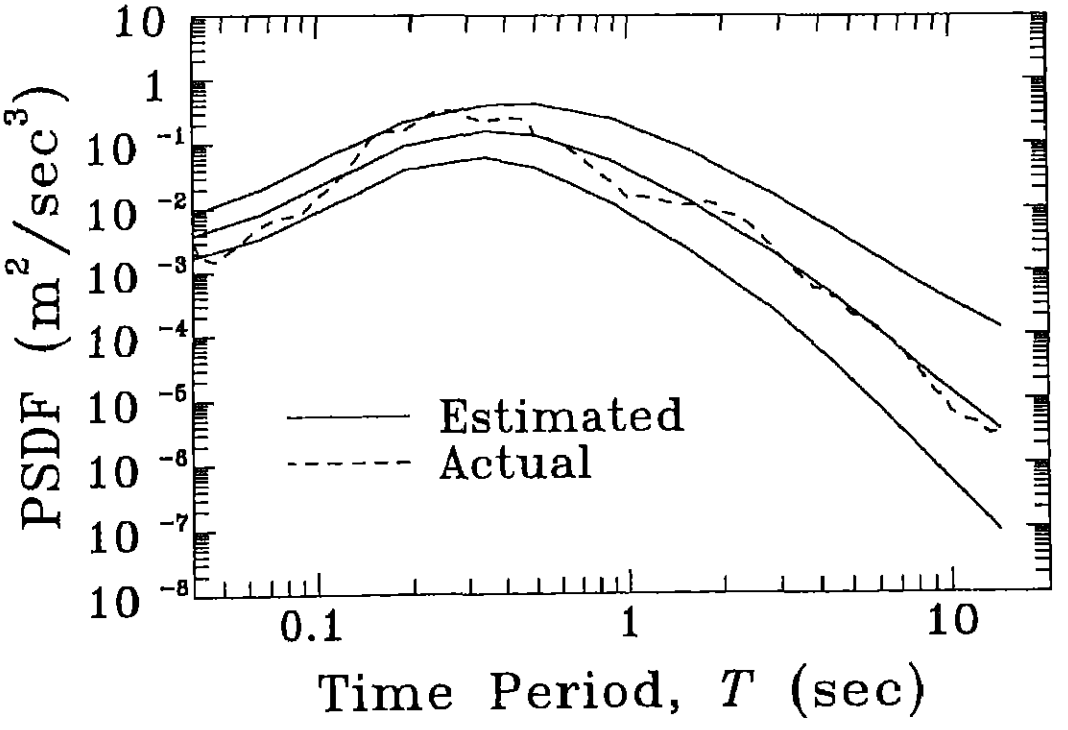

Figure 3.4(b) Comparison of Actual and Estimated PSDFs for Lytle Creek Earthquake Case.

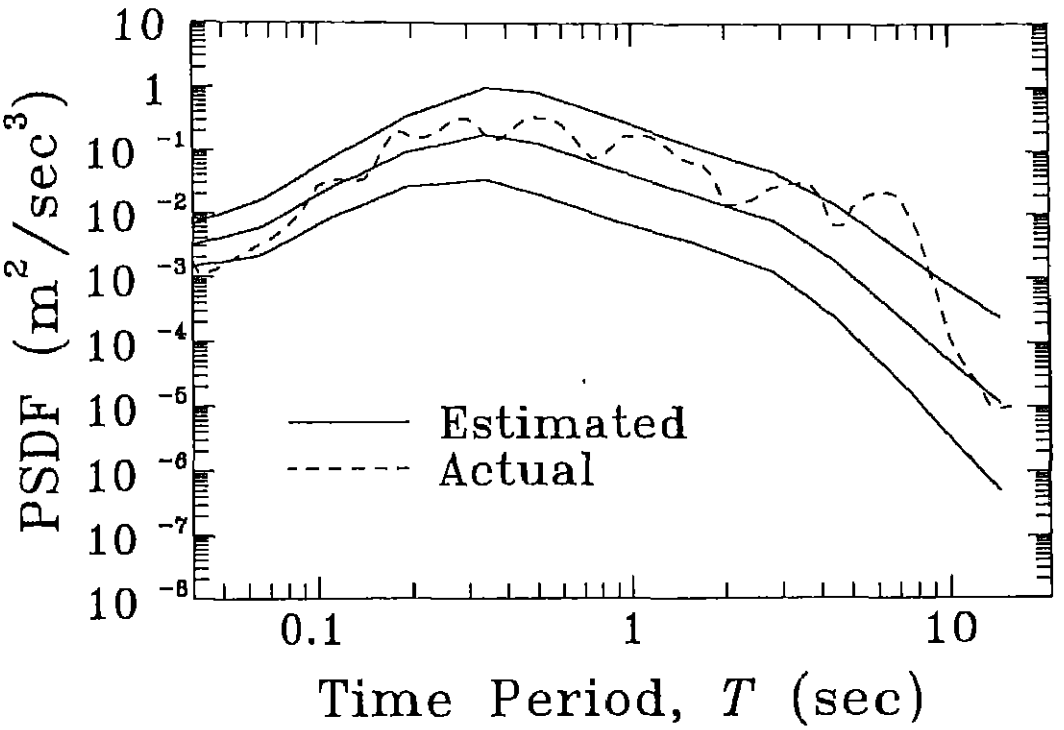

Figure 3.4(c) Comparison of Actual and Estimated PSDFs for San Fernando Earthquake Case.

and dashed lines representing the actual PSDFs. As in Chapter II, the estimated PSDFs have been obtained by using the least square estimates of the regression coefficients (along with the error estimates) at 12 time periods It may be seen that in all the three cases, the actual PSDFs lie within the 80% confidence intervals, while in the first two cases, those are in good agreement with the 50% confidence level estimates Here also, the 80% confidence interval is quite big, thus indicating the need to include more parameters in the scaling equation. It may however be observed that these confidence intervals are relatively narrower than those seen in Chapter II. Thus, it appears that the scaling relationship for the normalized PSDFs is slightly better. Further, it should be obvious from any of the Figs. 3 4(a) to 3.4(c) that the estimated PSDFs do not necessarily correspond to $1.0g$ of expected PGA, even though the regression analysis was based on the PSDFs corresponding to this much PGA Hence, the PSDF estimated by using the proposed scaling relationship should be properly scaled up or down depending upon whether the desired PGA level is more or less than the PGA corresponding to the estimated PSDF.

In order to see how the estimated PSDFs for different earthquake magnitudes compare with each other, four PSDFs curves have been estimated for M = 4 5, 5.5, 6.5 and 7.5 as shown in Fig. 3.5. For this, the least square estimates and error estimates corresponding to $p = 0.5$ as given in Tables 3.1(a) and 3.2(a) respectively have been used, and other parameters have been taken as $H = 5$ km and $R = 50$ km. Fig 3.5 clearly shows the increasing dominance of long period waves in the PSDFs for greater magnitudes. Similar trend is observed in Fig. 3.6 where the PSDF curves for $R = 25$, 50, 100 and 200 km have been compared with M, H and p respectively taken as 6.5, 5 km and 0 5. This is consistent with

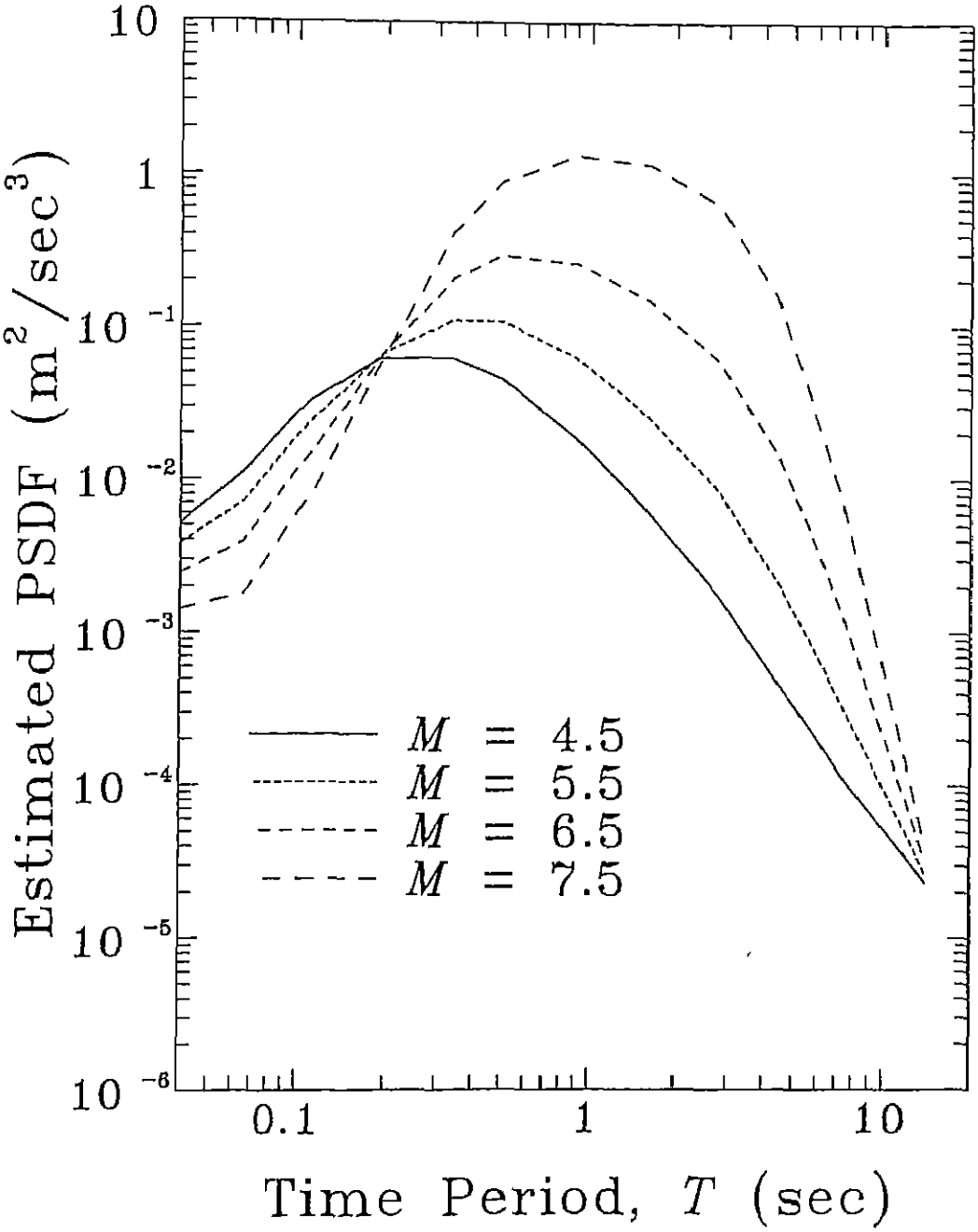

Figure 3.5 Comparison of Estimated PSDFs for Different Magnitudes in Case of Alluvium Site with $R = 50.0$ km, $H = 5.0$ km and $p = 0.5$.

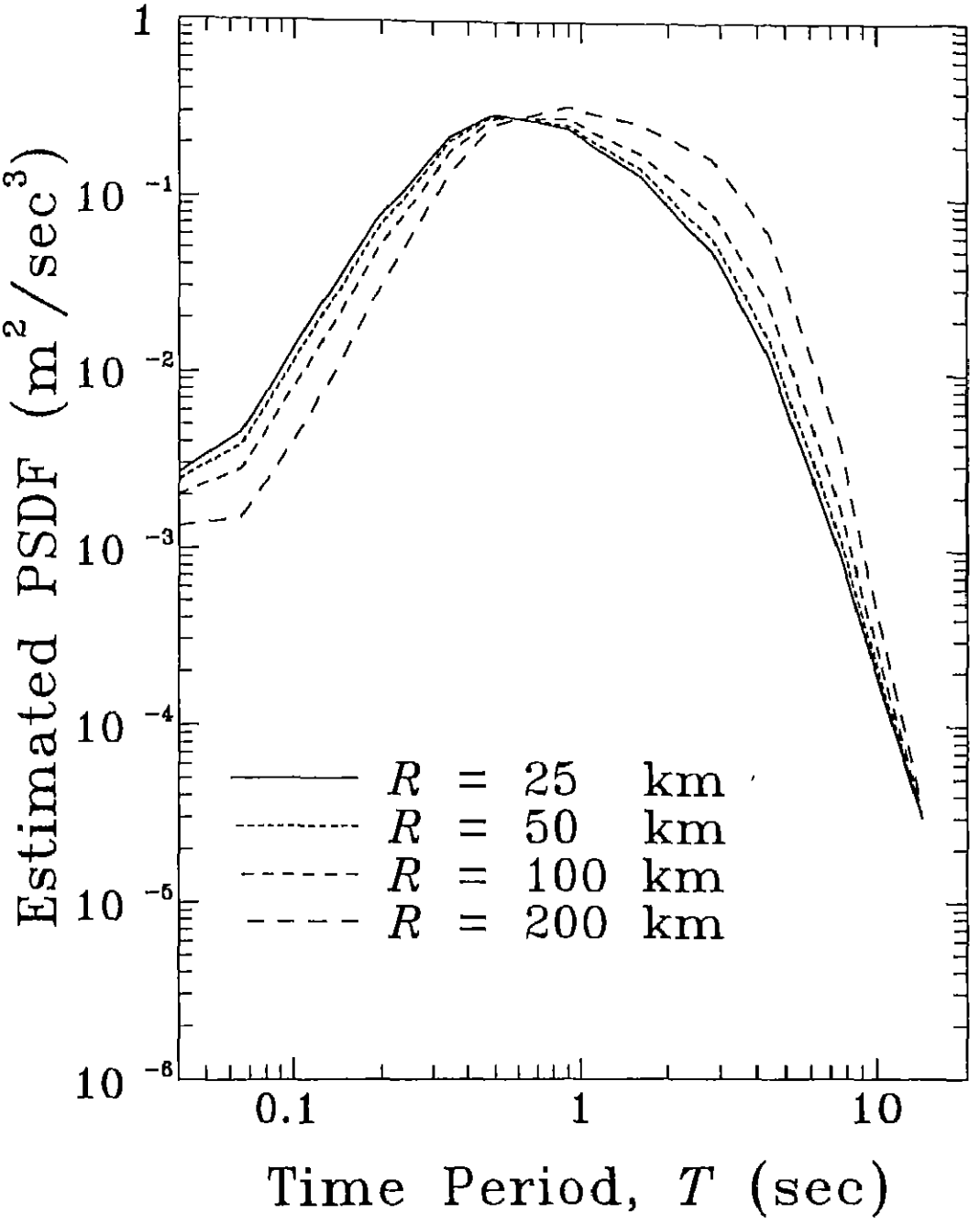

Figure 3.6 Comparison of Estimated PSDFs for Different Epicentral Distances in Case of Alluvium Site with $M = 6.5$, $H = 5.0$ km and $p = 0.5$.

the observation of Trifunac and Lee (1985b) that due to greater attenuation rate of high frequency waves, the motions recorded at large epicentral distances are richer in long period waves. Fig. 3.7 shows the effect of site conditions with the comparison of the PSDFs for alluvium, intermediate and hard rock site conditions. These PSDFs have been obtained for $M = 6.5$, $R = 50$ km, $H = 5$ km, and $p = 0.5$. It is seen that the PSDF for alluvium site condition has the peak at around 0.5 sec whereas the PSDF for the hard rock condition has the peak around 0.3 sec. This is also as expected since the ground periods in the alluvium site conditions are generally longer compared to the site conditions with little or no alluvium, and hence, the shorter period motions are filtered out during the dynamic response of the alluvium as an oscillator.

3.4 'Average' PSDF Shapes

The two models presented thus far for estimating the PSDF or normalized PSDF of earthquake ground motion are useful when the user is certain about the values of the governing parameters like magnitude, epicentral distance, focal depth etc. corresponding to the critical event. In those cases, however, where PGA value and the geologic site characteristics are the only information available, non-parametric simple and crude forms of PSDF curves may be quite useful. For this purpose, the raw PSDF data (i.e., the normalized PSDFs corresponding to $1.0g$ expected PGA and 20 sec duration) used for the regression analysis earlier in this chapter has been considered and an average curve has been obtained for each site condition. Fig. 3.8 shows the 'average' PSDFs for the three site conditions. These three PSDFs have also been normalized to correspond to $1.0g$ of expected PGA. It may be observed in the figure that except for a sharp peak in

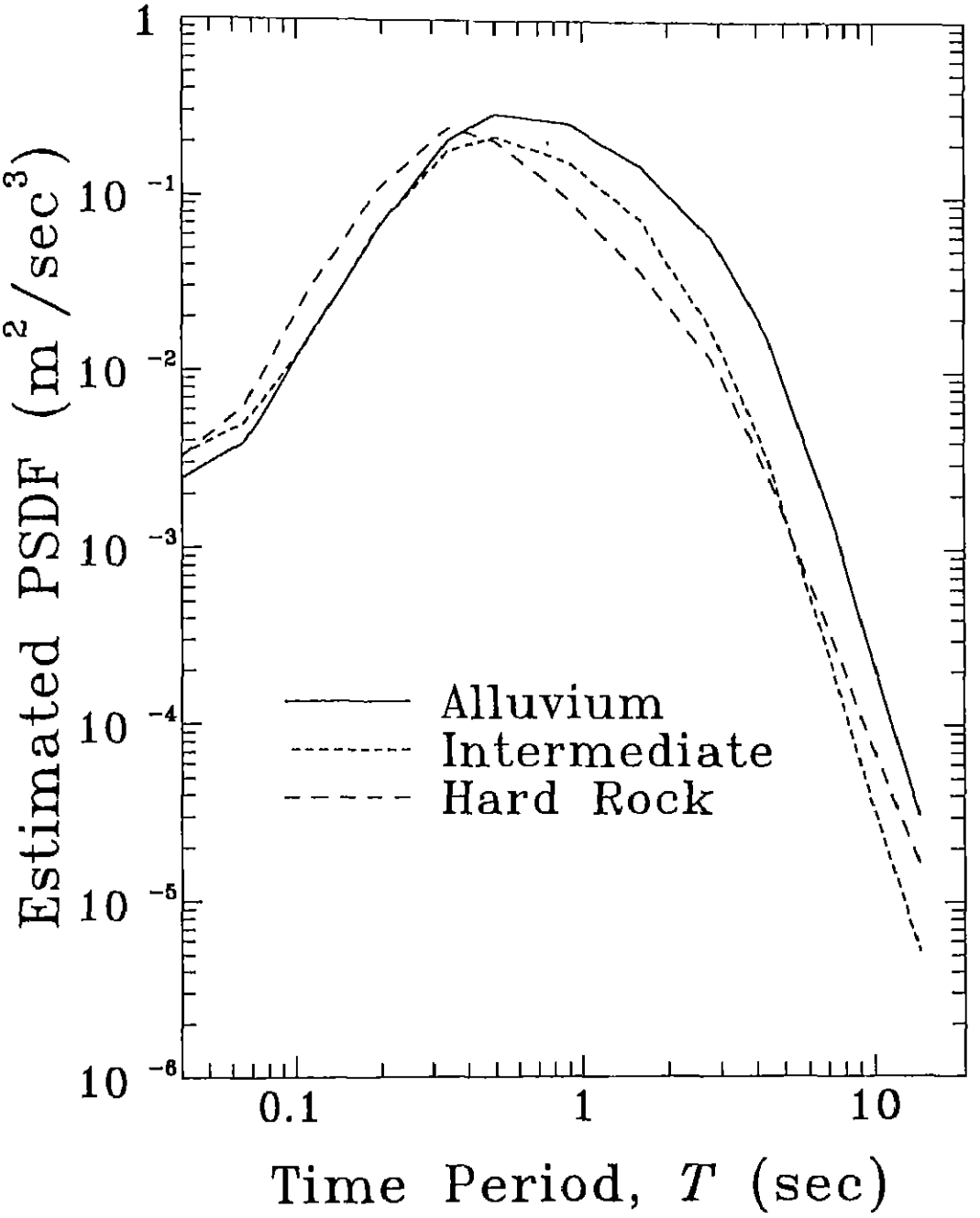

Figure 3.7 Comparison of Estimated PSDFs for Different Site Conditions with $M = 6.5$, $H = 5.0$ km and $p = 0.5$.

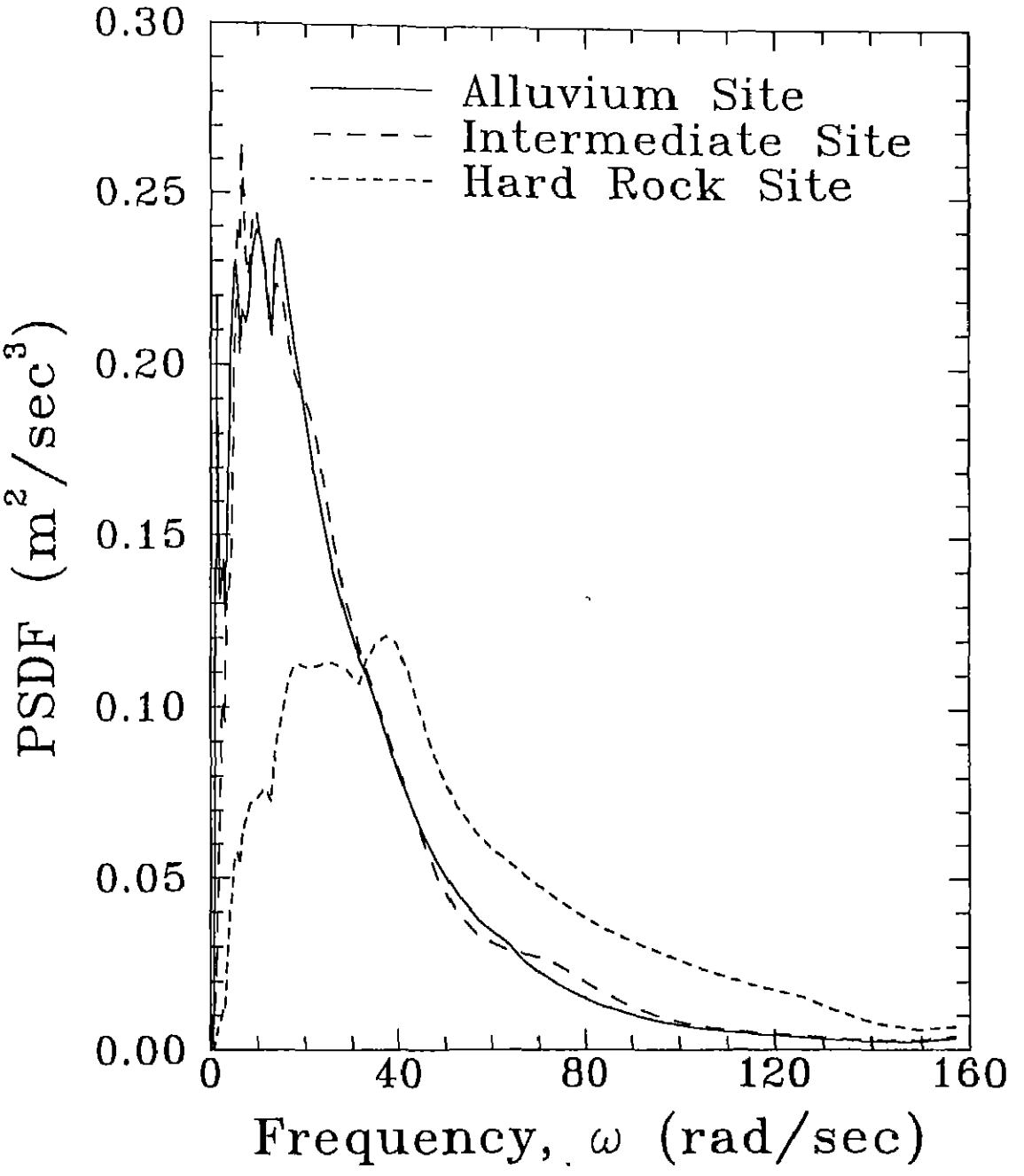

Figure 3.8 'Average' PSDF Curves for Different Site Conditions.

the low frequency range for the alluvium site case, the two curves corresponding to the alluvium and intermediate site conditions are in very good agreement. Both the curves show large and narrow-banded amplification of ground motions at high periods. The curve for hard rock site is seen to be quite different from these two curves as the peak in this curve has shifted towards higher frequency range and is much more flat. These trends are consistent with the lower values of ground period and higher values of ground damping usually adopted in the Kanai-Tajimi model, as the site approaches hard rock condition. These are also consistent with the trends reported in the previous regression analyses for FS spectra by Trifunac (1976b, 1979), and Trifunac and Lee (1985b) For the convenience of designers, the average $PSDF_N$ curves shown in Fig. 3.8 have been idealized by the following simple functional forms:

$$\begin{aligned} S(f) &= 3700f && 0.0 \le f < 0.60 \\ &= 2220 && 0.60 \le f < 2.30 \\ &= 2220\exp[-0.25(f-2.30)] && 2.30 \le f < 19.5 \\ &= 30.12 && 19.5 \le f \le 25.0 \end{aligned} \tag{3.8}$$

for alluvium and intermediate site conditions, and

$$\begin{aligned} S(f) &= 428f && 0.0 \le f < 2\,50 \\ &= 1070 && 2.50 \le f < 7.0 \\ &= 1070\exp[-0.167(f-7.0)] && 7\,0 \le f \le 25.0 \end{aligned} \tag{3.9}$$

for hard rock conditions. In Eqs. (3 8) and (3.9), f represents the frequency in Hz and $S(f)$ is the 'average' ground motion PSDF in cm^2/sec^3. It may be noted that both the functional forms correspond to $1\,0g$ of expected PGA with 20 sec ground motion duration. These forms have been compared with the actual 'average' curves in Figs. 3 9(a) and (b) respectively. It can be seen that the

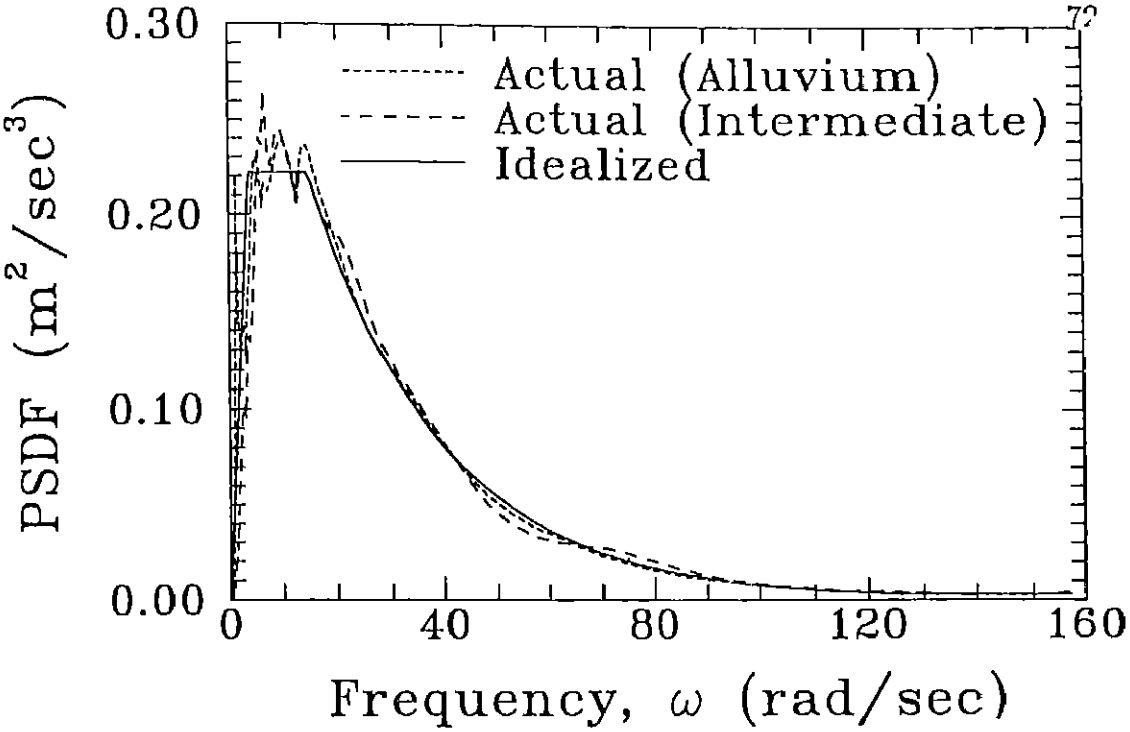

Figure 3.9(a) Comparison of Idealized and Actual PSDF Curves for Alluvium and Intermediate Site Conditions.

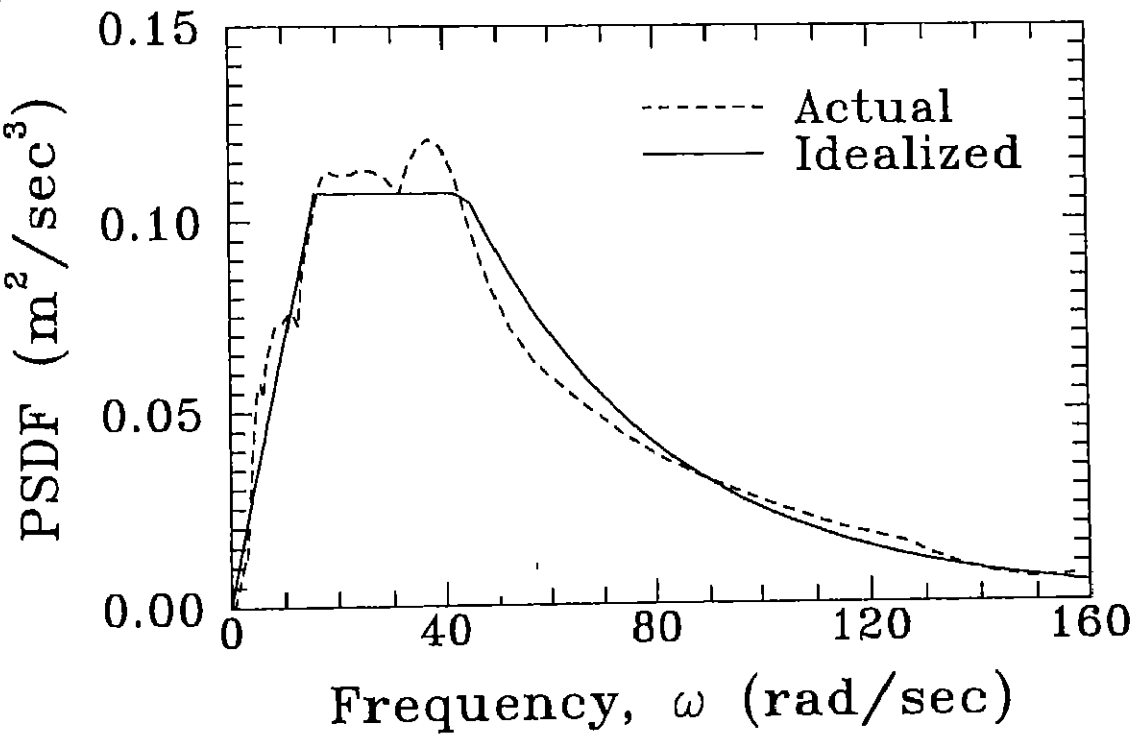

Figure 3.9(b) Comparison of Idealized and Actual PSDF Curves for Hard Rock Site Condition.

proposed PSDF curves for the two groups of site conditions are in very good agreement with the calculated 'average' PSDF curves.

CHAPTER IV

CONCLUSIONS

Two scaling models have been proposed in this study for the scaling of PSDF of horizontal ground motion in terms of earthquake magnitude, epicentral distance, focal depth These parameters can be conveniently obtained for practical applications. One of these models considers strong motion duration, as defined by Trifunac and Brady (1975b), also as a governing parameter. The other model has been proposed to estimate PSDF normalized to 20 sec of duration This model is useful where seismic hazard is specified in terms of PGA, and the desired PSDF has to be consistent with the specified value of PGA. Least square estimates of the regression coefficients and the residual estimates for different levels of confidence have been obtained based on the recorded motions in Western United States between 1931 and 1984 for alluvium, intermediate and hard rock site conditions. For obtaining crude estimates of normalized PSDF, when the knowledge of PGA and geologic site conditions only is available, simple and convenient functional relationships have also been suggested. It has been seen that the PSDFs estimated by proposed scaling relationships exhibit the effects of magnitude, epicentral distance and site conditions on the energy distribution as reported earlier. Also, in comparison with the duration-dependent model, the estimates from the model for normalized PSDF conform to a narrower range of variations for a given confidence interval However, both models need to consider greater number of source and propagation path related parameters for further reductions in this range.

The proposed models are likely to be very useful for PSDF-based risk assessment as the PSDFs estimated by these models can be assumed to correspond to equivalent stationary excitations In such applications, however, transient nature of response should be explicitly accounted for by using the available methods of analysis for SDOF and MDOF systems However, since the proposed relationships have been obtained from the data of western United States, those should be applied to other seismic regions of the world only with caution.

REFERENCES

Basu, B. and V.K. Gupta (1995) A probabilistic assessment of seismic damage in ductile structures, *Earthq. Eng. Struct. Dyn.*, **24**, 1333–1342

Bendat, J.S. and A.G Piersol (1986). Random Data Analysis and Measurement Procedures, *Wiley, New York, U S A.*

Blume, J.A. (1965). Earthquake ground motion and engineering procedures for important installations near active faults, *3rd Wld. Conf. Earthq. Eng., New Zealand*, **IV**, 53–67.

Bolt, B.A. (1973) Duration of strong ground motion, *5th Wld. Conf. Earthq Eng., Rome, Italy*, **6-D**.

Caughey, T.K and H.J. Stumpf (1961) Transient response of a dynamic system under random function, *J Appl. Mech. Div., ASME*, **28**(E), 563–566.

Chang, S.P., J.M. Seo, J. Kim, C H Yun and J R Lee (1991). Effects of PSDF forms on floor response spectra generation and direct solution methods, *Trans. 11th Struct. Mech. Reactor Tech.*, **K**, 255–260

Cloud, W.K. and V. Perez (1971) Unusual accelerograms recorded at Lima, Peru, *Bull. Seism. Soc. Amer.*, **61**, 633–640.

Clough, R W. and J. Penzien (1993). Dynamics of Structures, *McGraw-Hill, Singapore.*

Elghadamsi, F.E., B. Mohraz, C.T. Lee and P. Moayyad (1988). Time-dependent power spectral density of earthquake ground motion, *Soil Dyn. Earthq. Eng.*, **7**(1), 15–21.

Esteva, L. (1970). Seismic risk and seismic design decisions, in Seismic Design of Nuclear Power Plants (ed. R J. Hansen), *M.I.T Press, Cambridge, Massachusetts, U.S.A.*, 142–182.

Gupta, I.D. (1994). A probabilistic approach for computing the response of multi-degree-of-freedom structures, *Soil Dyn Earthq. Eng.*, **13**, 79–87.

Gupta, I.D. and R.G. Joshi (1993) On synthesizing response spectrum compatible accelerograms, *European Earthq. Eng.*, **VII(2)**, 25–33

Gupta, I.D., R.G. Joshi and V.K Pandit (1994). A note on design power spectral density function of strong earthquake ground motion, *10th Symp. on Earthq. Eng., Roorkee*, **II**, 843–852.

Gusev, A A. (1983). Descriptive statistical model of earthquake radiation and its application to an estimation of short-period strong motion, *Geophy J Royal Astro. Soc* , **74**, 787 -808.

Gutenberg, B. and C F. Richter (1942) Earthquake magnitude, intensity, energy and acceleration, *Bull. Seism. Soc. Amer.*, **32**, 163–191.

Gutenberg, B. and C F. Richter (1956) Earthquake magnitude, intensity, energy and acceleration, *Bull. Seism. Soc. Amer.*, **46**, 105–195

Hershberger, J. (1956). A comparison of earthquake acceleration with intensity ratings, *Bull. Seism. Soc. Amer.*, 46, 317–320.

Housner, G.W. (1965). Intensity of earthquake ground shaking near the causative fault, *3rd Wld. Conf. Earthq. Eng., New Zealand*, **III**, 94–111.

Ishimoto, M (1932). Echelle d' intensité sismique et acceleration maxima, *Bull. Earthq. Res. Inst., Univ. of Tokyo, Japan*, **10**, 614–626.

Kanai, K. (1957) Semi-empirical formula for the seismic characteristics of the ground, *Bull. Earthq. Res. Inst., Univ. of Tokyo, Japan*, **35**, 309–325

Kanai, K. (1966). Improved empirical formula for characteristics of stray earthquake motions, *Proc. Japan Earthq. Symp.*, 1–4

Kaul, M K (1978) Stochastic characterization of earthquake through their response spectrum, *Earthq. Eng. Struct. Dyn* , **6**, 497–509.

Kawashima, K. and K. Aiwaza (1989). Bracketed and normalized durations of earthquake ground accleration, *Earthq. Eng. Struct. Dyn.*, **18**, 1041–1051.

Kawasumi, H. (1951). Measures of earthquake danger and expectancy of maximum intensity throughout Japan as inferred from the seismic activity in historical times, *Bull. Earthq. Res. Inst., Univ. of Tokyo, Japan*, **29**, 469–482

Lai, S.P. (1982). Statistical characterization of strong ground motions using power spectral density function, *Bull. Seism. Soc. Amer.*, **72(1)**, 259–274.

Lee, V.W. (1987). Influence of local soil and geologic site conditions on pseudo relative velocity spectrum amplitudes of recorded strong motion accelerations, *Rep. No. CE 87–06, Dept. of Civil Eng., Univ. of Southern California, Los Angeles, California, U.S.A.*

Lee, V.W and M.D. Trifunac (1987). Strong earthquake ground motion data in EQUINFOS: part 1, *Rep. No. CE 87–01, Dept. of Civil Eng., Univ. of Southern California, Los Angeles, California, U.S.A.*

Lee, V W., M D. Trifunac, M I Todorovska and E I Novikova (1995). Empirical equations describing attenuation of peaks of strong ground motion, in terms of magnitude, distance, path effects and site conditions, *Rep. No. CE 95-02, Dept. of Civil Eng., Univ. of Southern California, Los Angeles, California, U.S A.*

Lin, Y K and Y. Yong (1987). Evolutionary Kanai-Tajimi earthquake models, *J. Eng. Mech. Div. (ASCE)*, **113(8)**, 1119-1137.

Liu, S.C. (1970). Evolutionary power spectral density of strong motion earthquakes, *Bull. Seism. Soc. Amer.*, **60**, 891–900

McCann, M.W. and H.C. Shah (1979). Determining strong-motion duration of earthquakes, *Bull. Seism. Soc. Amer.*, **69**, 1253–1265.

Medvedev, S.V. and W. Sponheuer (1969). Scale of seismic intensity, *Proc 4th Wld. Conf. Earthq Eng., Santiago, Chile*, **A-2**, 143–153

Milne, W.G. and A.G. Davenport (1969) Distribution of earthquake risk in Canada, *Bull. Seism. Soc. Amer.*, **59**, 754–779.

Mohraz, B and M.M. Peng (1989). Use of a low-pass filter in determining the duration of strong ground motion, *J. Pressure Vessels Piping, ASME*, **182**, 197–200.

Neumann, F. (1954). Earthquake Intensity and Related Ground Motion, *Univ. Press, Seattle, Washington, U S.A.*

Novikova, E.I. and M D. Trifunac (1994) Duration of strong ground motion in terms of the earthquake magnitude, epicentral distance, site conditions and site geometry, *Earthq. Eng. Struct Dyn.*, **23**, 1023–1043.

Okamoto, S. (1973). Introduction to Earthquake Engineering, *John Wiley, New York, U.S.A.*

Page, R.A., D.M. Boore, W.B. Joyner and H.W. Coulter (1972). Ground motion values for use in the seismic design of the Trans-Alaska pipeline system, *Circular 672, U.S. Geological Survey, Washington, D.C., U.S A.*

Pfaffinger, D.D. (1983). Calculation of power spectra from response spectra, *J. Eng. Mech. Div. (ASCE)*, **109(1)**, 357–372.

Richter, C.F. (1958). Elementary Seismology, *Freeman & Co., San Francisco, California, U.S.A.*

Savarensky, Y.F. and D.P. Kirnos (1955). Elements of Seismology and Seismometry, *Moscow, Russia.*

Schnabel P. and H B Seed (1973) Accelerations in rock for earthquakes in the western United States, *Bull Seism. Soc. Amer* , **63**, 501–516.

Seed, H.B., C. Ugas and J Lysmer (1976). Site-dependent spectra for earthquake -resistant design, *Bull. Seism. Soc. Amer.*, **66**, 221–243

Shinozuka, M. (1970) Random processes with evolutionary power, *J. Eng. Mech. Div., Proc. ASCE*, **96(EM4)**, 543–545.

Shrikhande, M and V.K. Gupta (1996). On generating ensemble of design spectrum-compatible accelerograms, *European Earthq Eng.*, (in press)

Spanos, P.D and L M. Vargas Loli (1985). A statistical approach to generation of design spectrum compatible earthquake time histories, *Soil Dyn Earthq Eng* , **4(1)**, 2–8.

Sundararajan, C. (1980). An iterative method for the generation of seismic power spectral density functions, *Nucl. Eng. Des.*, **61**, 13–23.

Tajimi, H. (1960) A standard method of determining the maximum response of a building structure during an earthquake, *Proc. Second Wld. Conf Earthq. Eng., Tokyo, Japan*, **II**.

Todorovska, M.I. (1994) Order statistics of functionals of strong ground motion for a class of renewal processes, *Soil Dyn. Earthq. Eng* , **13**, 399–405.

Trifunac, M.D. (1976a). Preliminary analysis of the peaks of strong earthquake ground motion—dependence of peaks on earthquake magnitude, epicentral distance and recording site conditions, *Bull. Seism. Soc. Amer.*, **66**, 189–219.

Trifunac, M.D. (1976b) Preliminary empirical model for scaling Fourier amplitude spectra of strong ground acceleration in terms of earthquake magnitude, source to station distance and recording site conditions, *Bull. Seism. Soc. Amer.*, **68**, 1345–1373.

Trifunac, M.D. (1987). Influence of local soil and geologic site conditions on Fourier amplitude spectrum amplitudes of recorded strong motion accelerations, *Rep. No. CE 87–04, Dept. of Civil Eng., Univ. of Southern California, Los Angeles, California, U.S.A*

Trifunac, M.D. (1992). Should peak accelerations be used to scale design spectrum amplitudes? *Proc. 10th Wld Conf. Earthq. Eng., Madrid, Spain*, **10**, 5817–5822.

Trifunac, M.D. and J.G. Anderson (1977). Preliminary empirical models for scaling absolute acceleration spectra, *Rep. No. CE 77–03, Dept. of Civil Eng., Univ. of Southern California, Los Angeles, California, U.S.A.*

Trifunac, M.D. and J G Anderson (1978). Preliminary empirical models for scaling pseudo relative velocity spectra, *Rep No. CE 78–04, Dept. of Civil Eng., Univ. of Southern California, Los Angeles, California, U.S.A.*

Trifunac, M.D. and A.G Brady (1975a) On the correlation of seismic intensity scales with the peaks of recorded strong ground motion, *Bull Seism Soc. Amer.*, 65, 139–162

Trifunac, M.D. and A.G. Brady (1975b). A study on the duration of strong earthquake ground motion, *Bull. Seism. Soc. Amer.*, 65, 581–626.

Trifunac, M.D. and A.G. Brady (1976). Correlation of peak acceleration, velocity and displacement with earthquake magnitude, distance and site contitions, *Earthq. Eng. Struct. Dyn.*, 4, 455–471.

Trifunac, M D. and V.W. Lee (1978). Dependence of the Fourier amplitude spectra of strong motion acceleration on the depth of sedimentary deposits, *Rep. No. CE 78–14, Dept. of Civil Eng., Univ. of Southern California, Los Angeles, California, U.S.A.*

Trifunac, M.D. and V.W. Lee (1979). Dependence of pseudo relative velocity spectra of strong motion acceleration on the depth of sedimentary deposits, *Rep. No. CE 79–02, Dept. of Civil Eng., Univ. of Southern California, Los Angeles, California, U.S.A.*

Trifunac, M.D. and V.W. Lee (1985a). Frequency-dependent attenuation of strong earthquake ground motion, *Rep. No. CE 85–02, Dept. of Civil Eng., Univ. of Southern California, Los Angeles, California, U.S A.*

Trifunac, M.D. and V.W. Lee (1985b) Preliminary empirical model for scaling Fourier amplitude spectra of strong ground acceleration in terms of earthquake magnitude, source to station distance, site intensity and recording site conditions, *Rep. No. CE 85–03, Dept. of Civil Eng., Univ. of Southern California, Los Angeles, California, U.S.A.*

Trifunac, M.D. and V.W. Lee (1985c). Preliminary empirical model for scaling pseudo relative velocity spectra of strong earthquake acceleration in terms of earthquake magnitude, source to station distance, site intensity and recording site conditions, *Rep. No. CE 85–04, Dept. of Civil Eng., Univ. of Southern California, Los Angeles, California.*

Trifunac, M.D. and B.D Westermo (1982). Duration of strong earthquake shaking, *Soil Dyn. Earthq. Eng.*, 2, 117–121.

Udwadia, F.E. and M.D. Trifunac (1974). Characterization of response spectra through the statistics of oscillator response, *Bull. Seism. Soc. Amer.*, 64, 205–219.

Unruh, J F. and D D. Kana (1981) An iterative procedure for the generation of consistent power/response spectrum, *Nucl. Eng Des* , **66**, 427–435

Vanmarcke, E H. and S.P. Lai (1980) Strong-motion duration and rms amplitude of earthquake records, *Bull. Seism. Soc. Amer.*, **70**, 1293–1307.

Westermo, B D. and M.D. Trifunac (1978). Correlations of the frequency dependent duration of strong earthquake ground motion with the magnitude, epicentral distance, and the depth of sediments at the recording site, *Rep No. CE 78-12, Dept. of Civil Eng., Univ. of Southern California, Los Angeles, California.*

Date Slip

This book is to be returned on the date last stamped

A 123652

CE-1997-M-DE-PRE